PHOTOCHEMICAL & THERMOCHEMICAL SPLITTING OF WATER

C.N.R. RAO

Jawaharlal Nehru Centre for Advanced Scientific Research

Indian Institute of Science

International Centre for Materials Science
Bangalore, India

Redox Reaction in Water Splitting

Oxidation: $2H_2O \longrightarrow O_2 + 4H^+ + 4e^-$ (1.23 V *vs.* SHE)

Reduction: $4H^+ + 4e^- \longrightarrow 2H_2$ (0.0 V *vs.* SHE)

$$\mathbf{2H_2O \longrightarrow O_2 + 2H_2}$$

- **ΔG of water splitting reaction is positive**
- **Energy intensive process**
- ***Oxidation of water involves 4e⁻ and is thermodynamically more challenging***

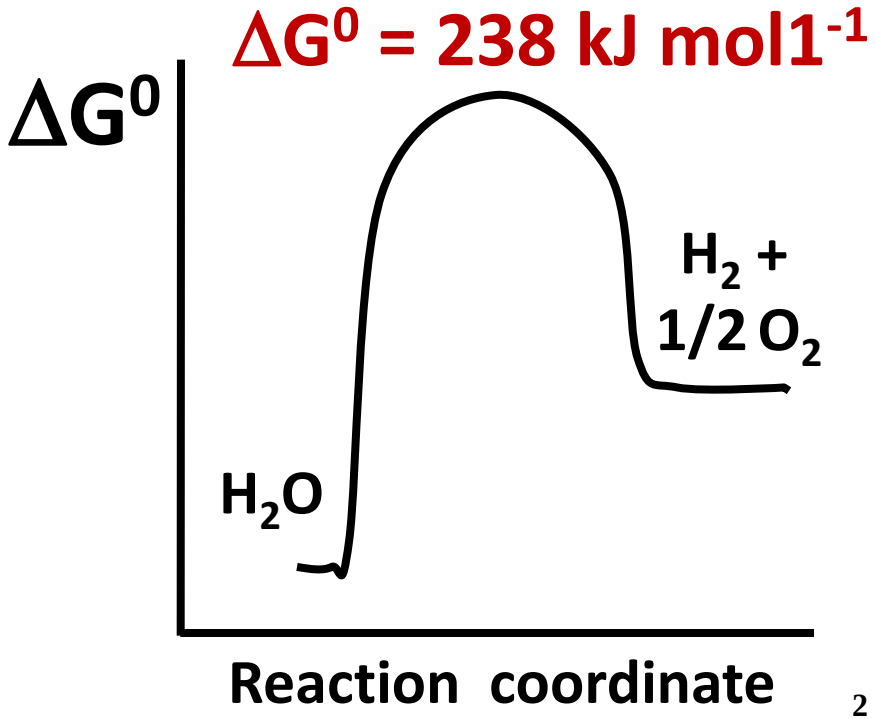

Classification of Water Splitting Processes

Energy		**Process**
Light	=>	**Photo-catalytic**
Electrical	=>	**Electrochemical**
Light + Electrical	=>	**Photo- electrochemical**

Mechanism

1. Artificial Photosynthesis
2. Water splitting using – semiconductors *etc.*

Natural photosynthesis

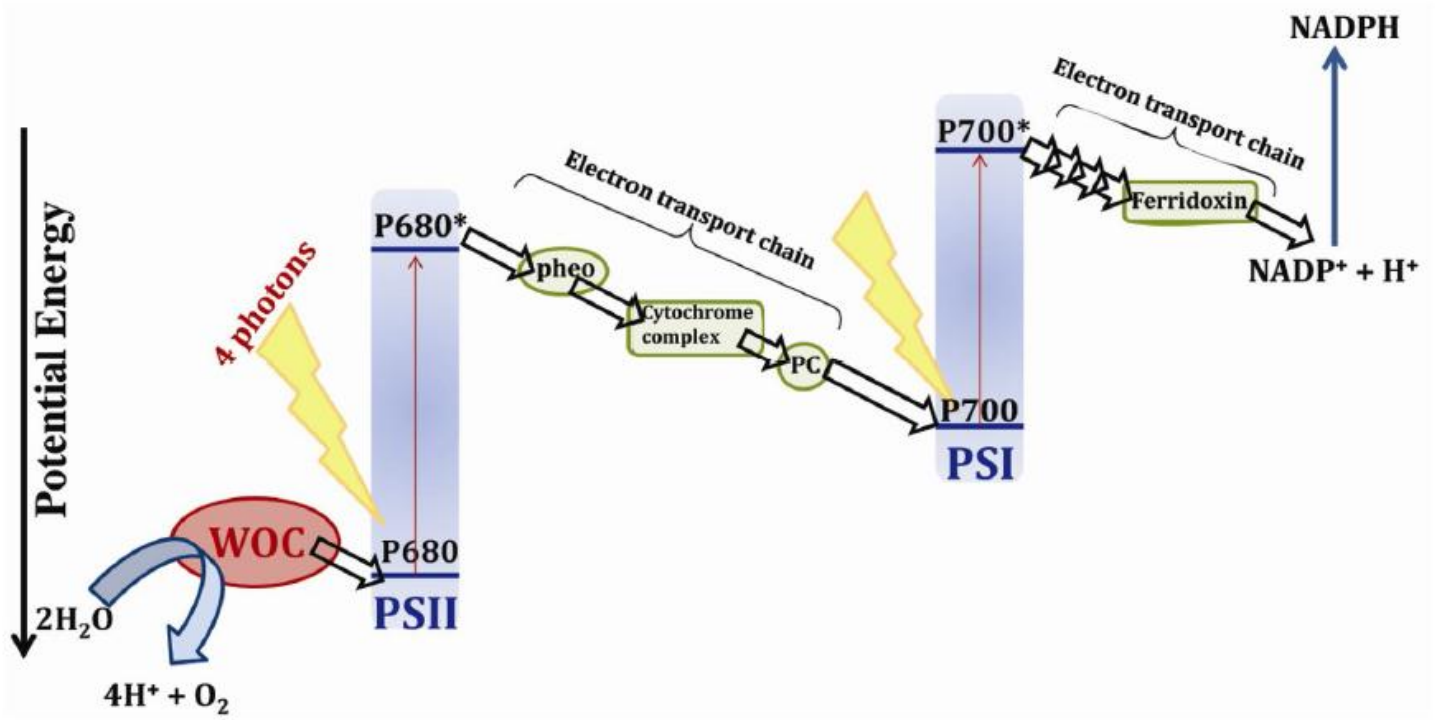

i. Absorption of light by PSII & generation of e^-

ii. Cascade of downhill movement of e^- along very closely spaced energy levels to PSI and h+ used up for H_2O oxidation -100% charge seperation

iii. Photoexcitation of PSI

iv. Downhill movement of e- and donation of e^- to $NADP^+$

v. 2 photons give one e^- and one h^+

Mechanism of Photosynthesis

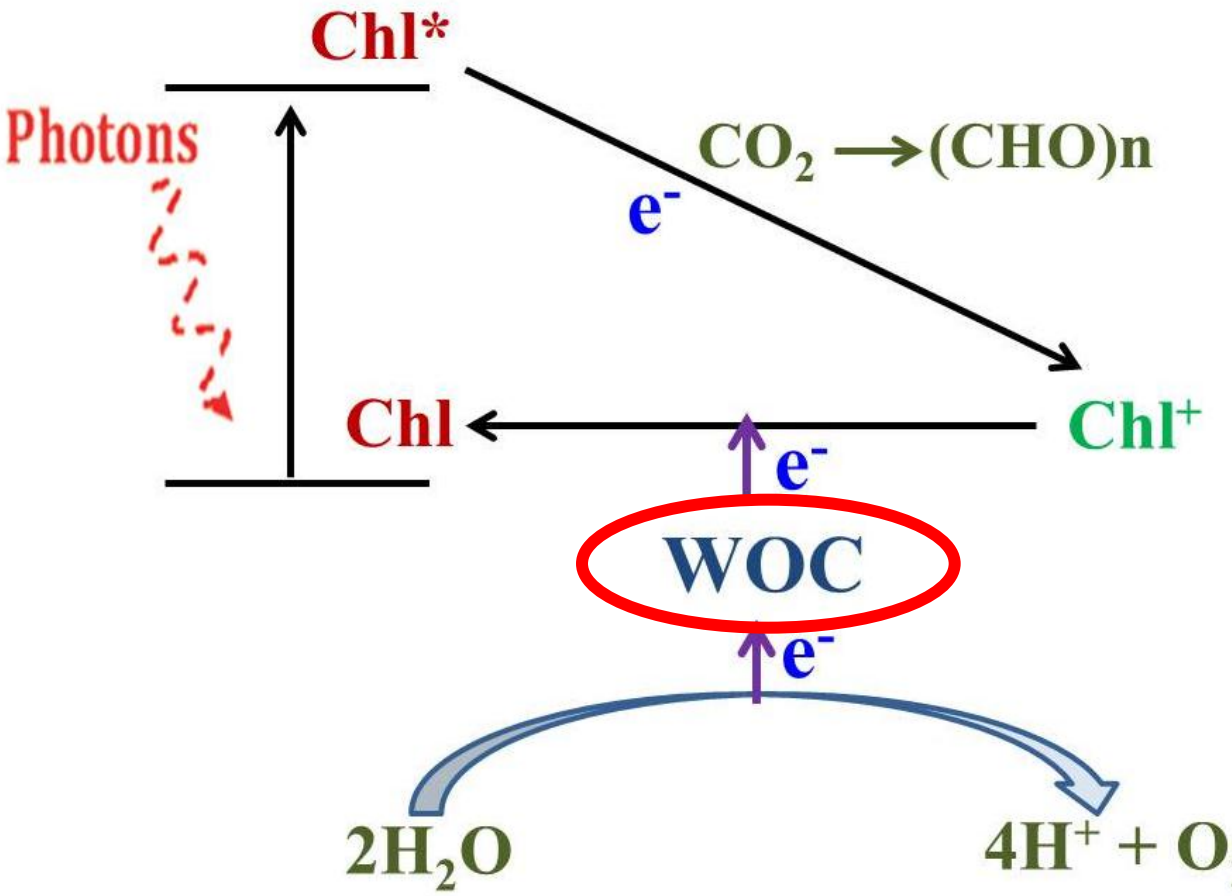

WOC = Water Oxidation Complex

Mechanism of Artificial Photosynthesis

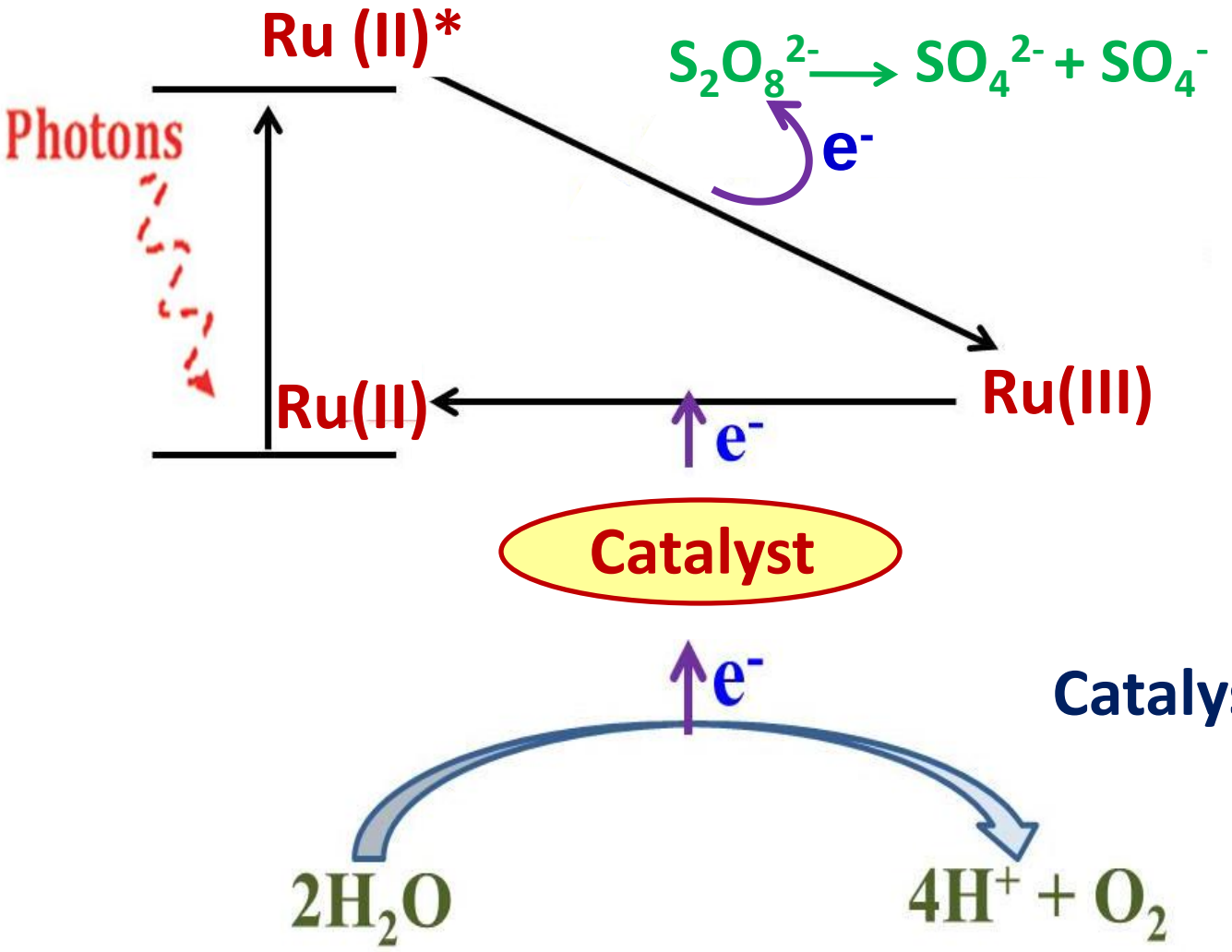

Catalyst => M^{n+} / $M^{(n+1)+}$

Photosynthetic center in plants

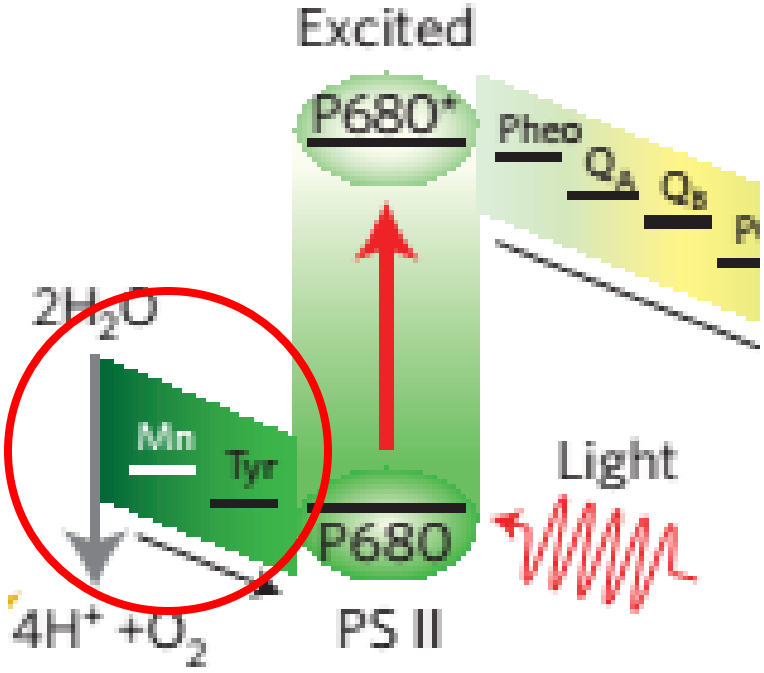

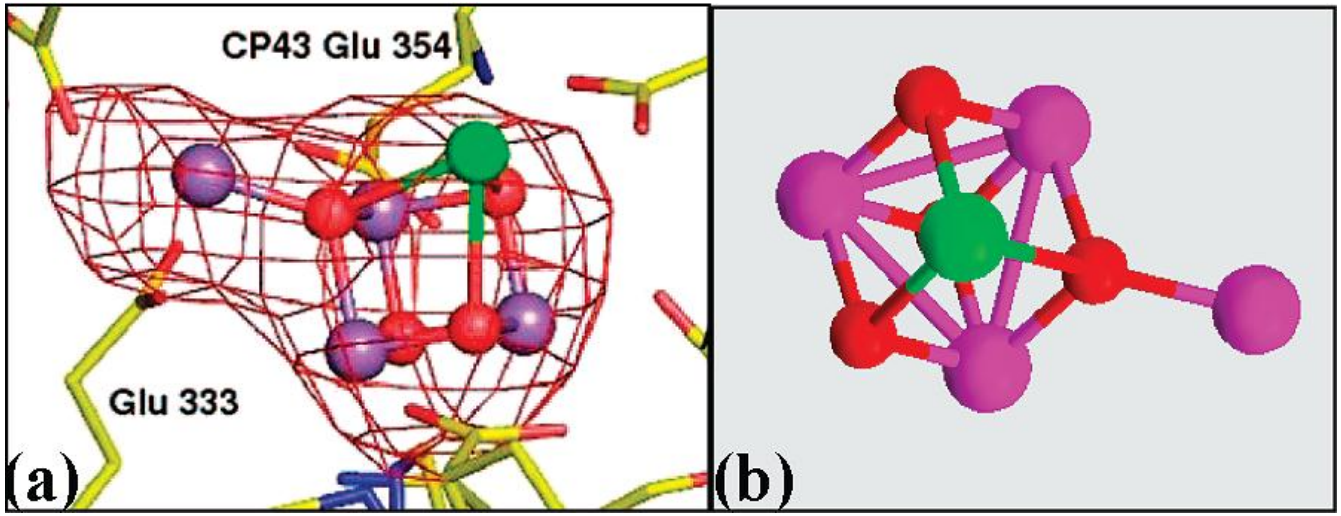

Mn_4CaO_4 ***core main component of* PSII**

Photocatalytic activity in oxide with Mn_4O_4 cubane

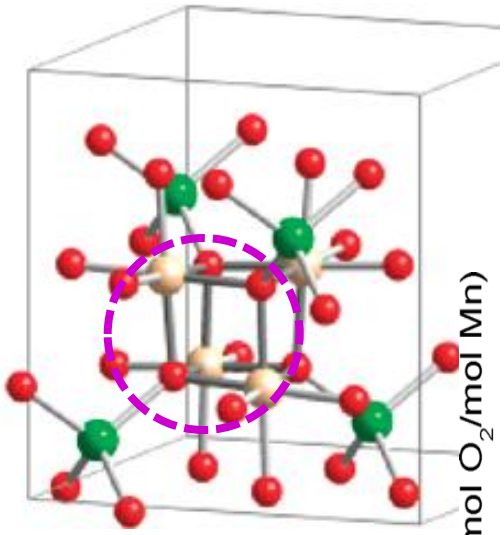

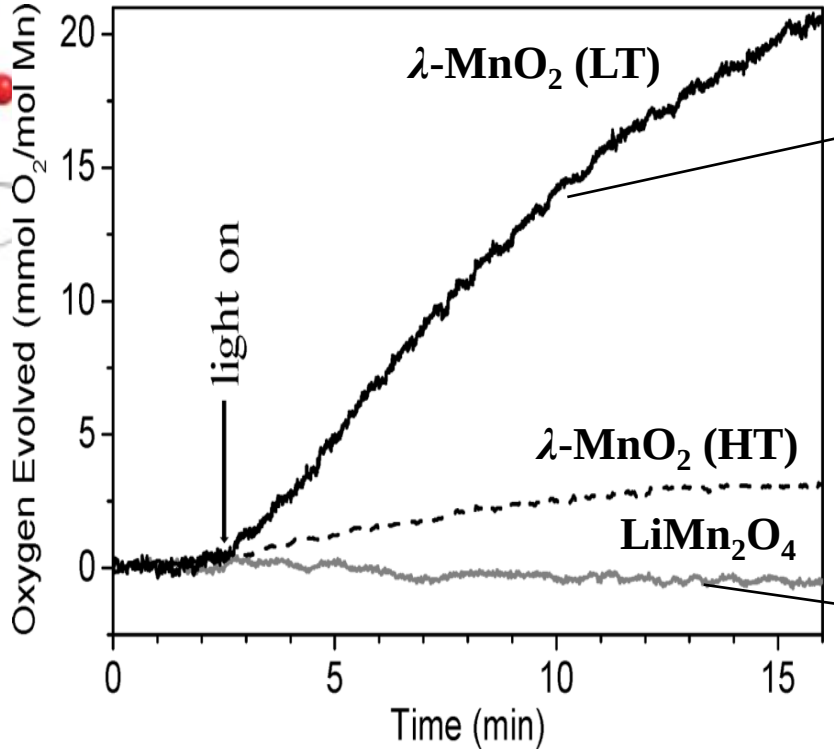

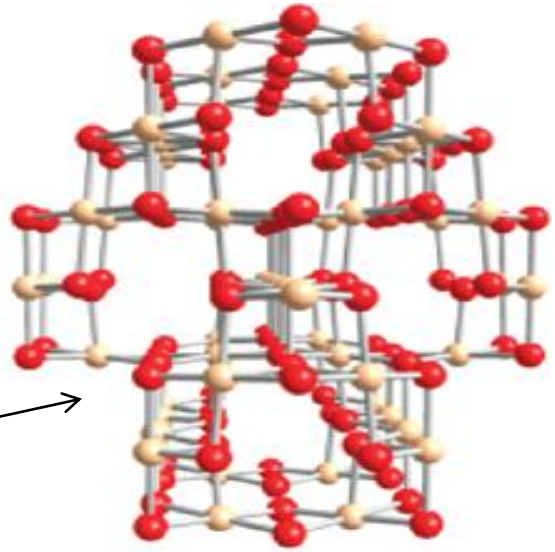

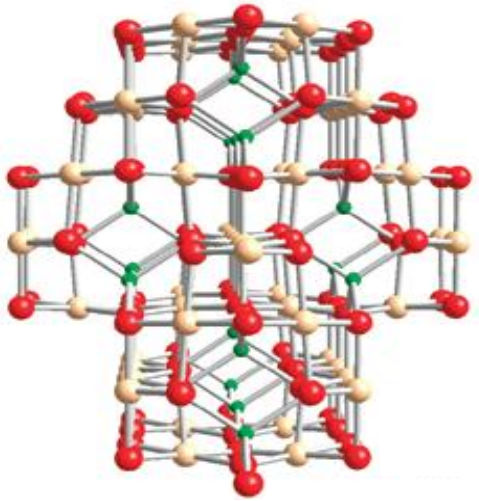

Greenbaltt and coworkers, J. Am. Chem. Soc. , **2010**, 132**,** 11467

$LiMn_2O_4$ and effect of delithiation

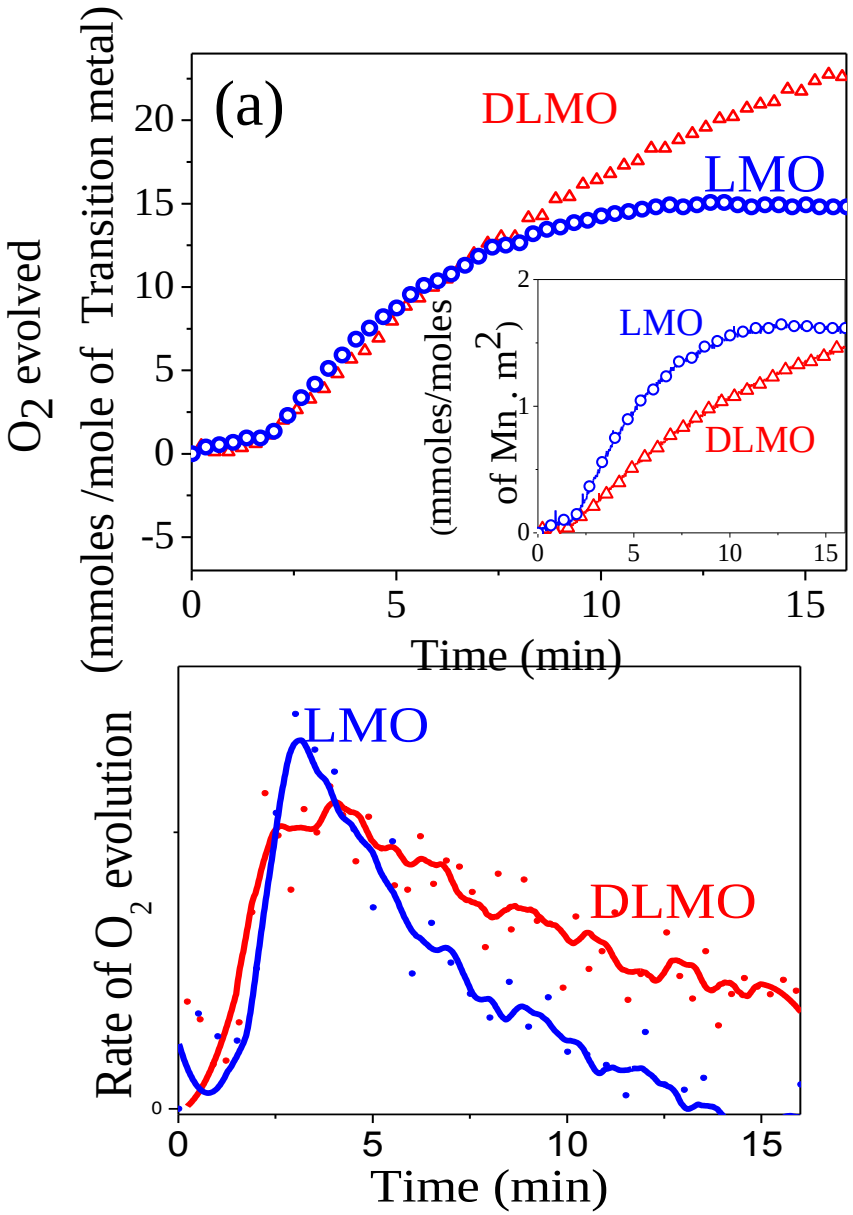

LMO = $LiMn_2O_4$; Mn(III/IV)

DLMO = Delithiated LMO ; Mn(IV)

- ***O_2 evolution increases only slightly on delithiation***
- ***O_2 evolved per unit surface area is higher for LMO***
- ***Rate of O_2 evolved is slightly high for LMO***
- ***Turn over frequency (TOF)***

LMO =2.2×10^{-5} s^{-1} & DLMO = 2×10^{-5} s^{-1}

U. Maitra, B. S. Naidu, A. Govindaraj, and C. N. R. Rao. Proc. Natl. Aacd. Sci., USA, **2013**, 110, 11704–11707

Importance of Co (III) and Mn (III)

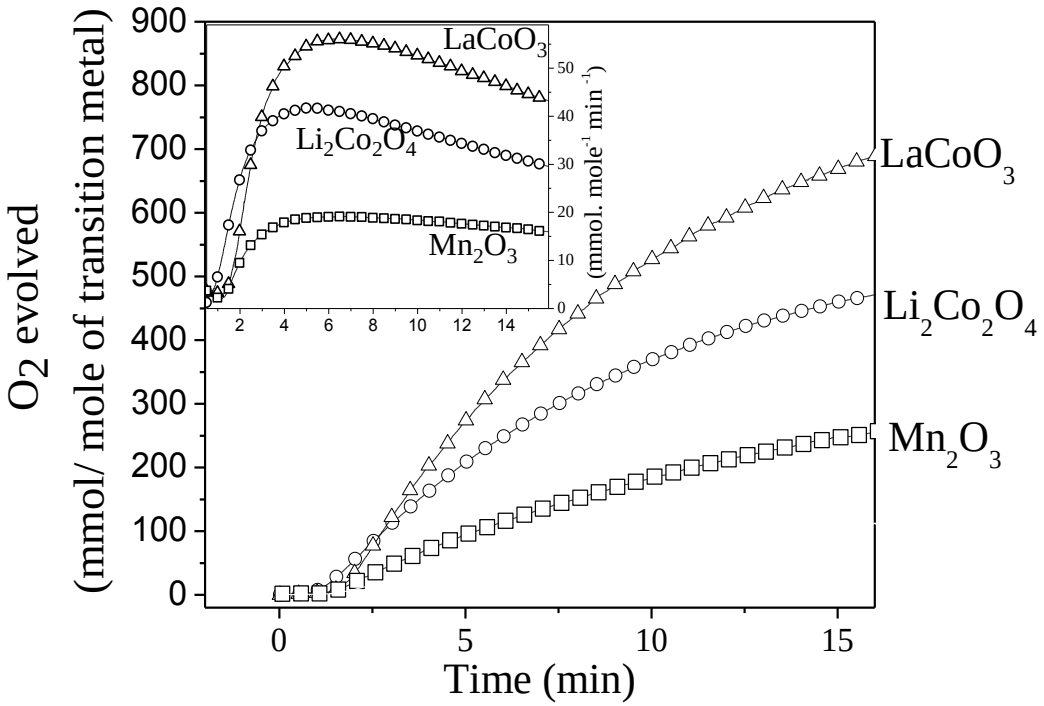

Sample	Structure	TOF (s^{-1})
$Li_2Co_2O_4$	Spinel	9×10^{-4}
$LaCoO_3$	Perovskite	1.4×10^{-3}
Mn_2O_3	Bixbyite	5×10^{-4}
$LaMnO_3$	Perovskite	4.8×10^{-4}
$MgMn_2O_4$	Spinel	8.2×10^{-5}

All samples with Co (III) and Mn (III) & e_g^1 , irrespective of crystal structure show good catalytic activity for O_2 evolution

O_2 evolution by $LnMnO_3$

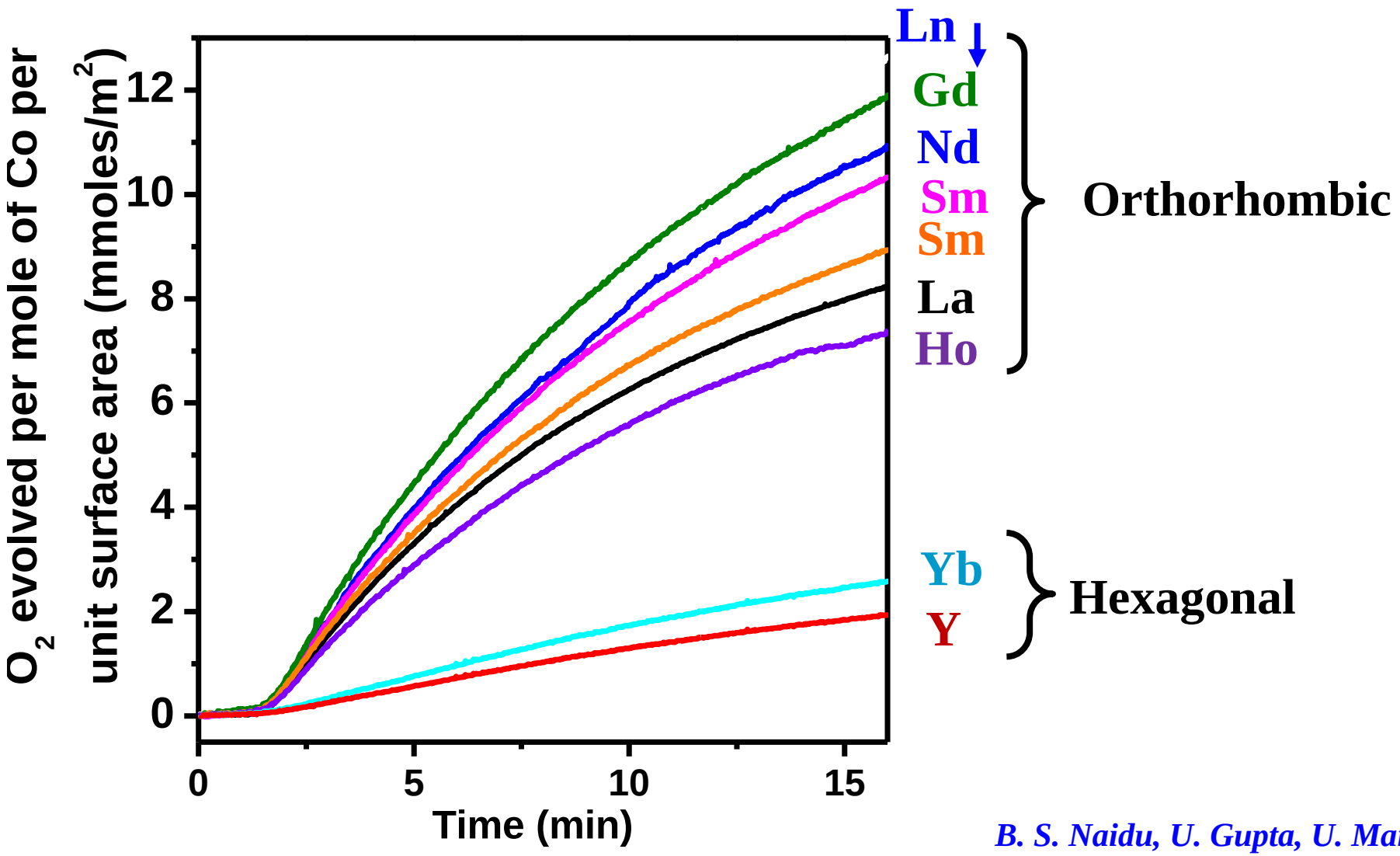

B. S. Naidu, U. Gupta, U. Maitra and C. N. R. Rao, Chem. Phys. Lett. 2014, 591, 277–281.

O_2 evolution by $LnCoO_3$

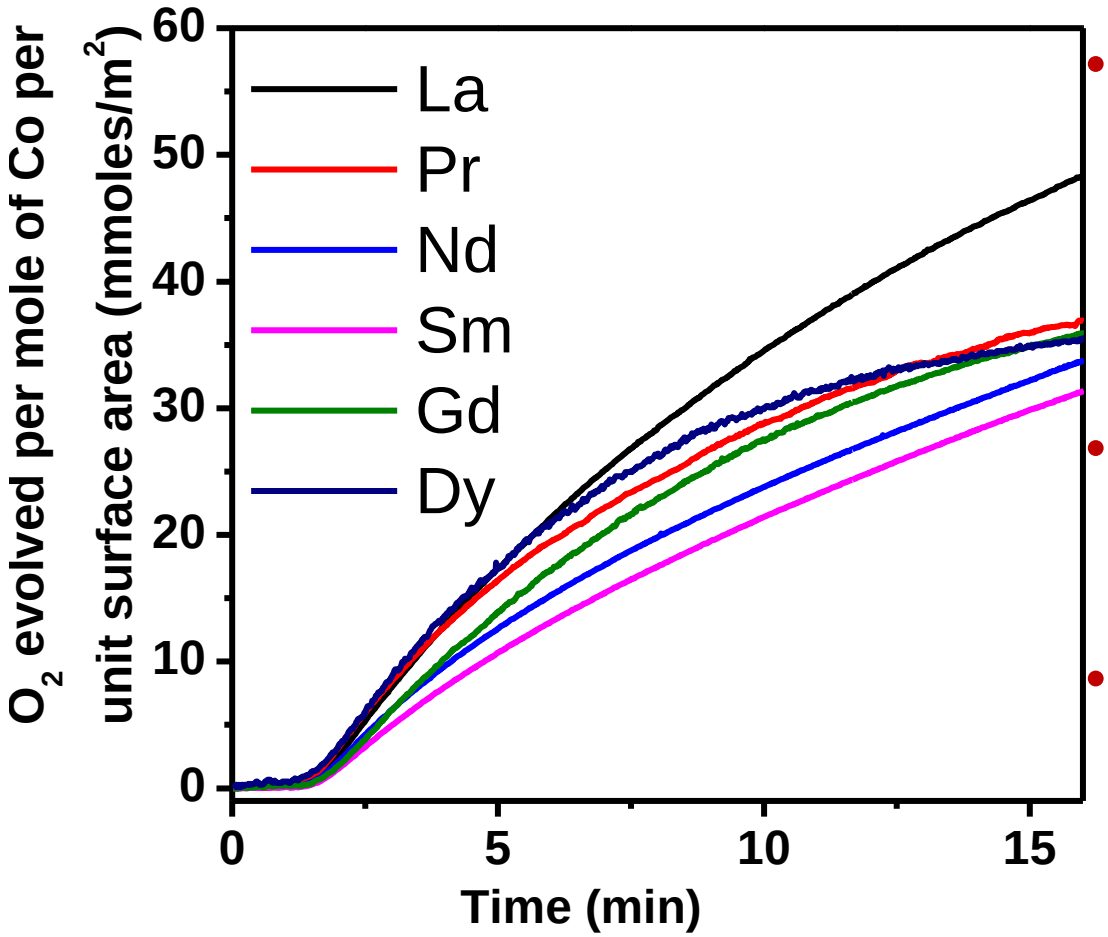

- ***All orthorhombic perovskites with Co (III) show comparable catalytic activity for O_2 evolution***
- ***$LaCoO_3$ shows slightly higher activity.***
- ***TOF is comparable to other perovskites.***

Conclusions

- ***All Mn and Co oxides in +3 oxidation state show good catalytic activity irrespective of their crystal structure.***
- ***Trivalency ensures easy electron transfer from the metal ion***
- ***For good catalytic activity B site transition metal ions must have 1 electron in antibonding e_g orbital (eg. d^4 and d^6 systems).***
- ***Localized e_g electron in the antibonding σ^* can readily be donated during the photocatalytic OER***
- ***Presence of a single electron in the antibonding e_g orbital is expected to yield just the appropriate strength of interaction between O_2 and the catalyst.***

U. Maitra, B. S. Naidu, A. Govindaraj, and C. N. R. Rao. **Proc. Natl. Aacd. Sc., USA,** 2013, **110**, 11704–11707.

B. S. Naidu, U. Gupta, U. Maitra and C. N. R. Rao, **Chem. Phys. Lett**. 2014, **591**, 277–281.

Enhanced O_2 evolution of $LaCoO_3$ and $LaMnO_3$ with Pt nanoparticles as electron channel

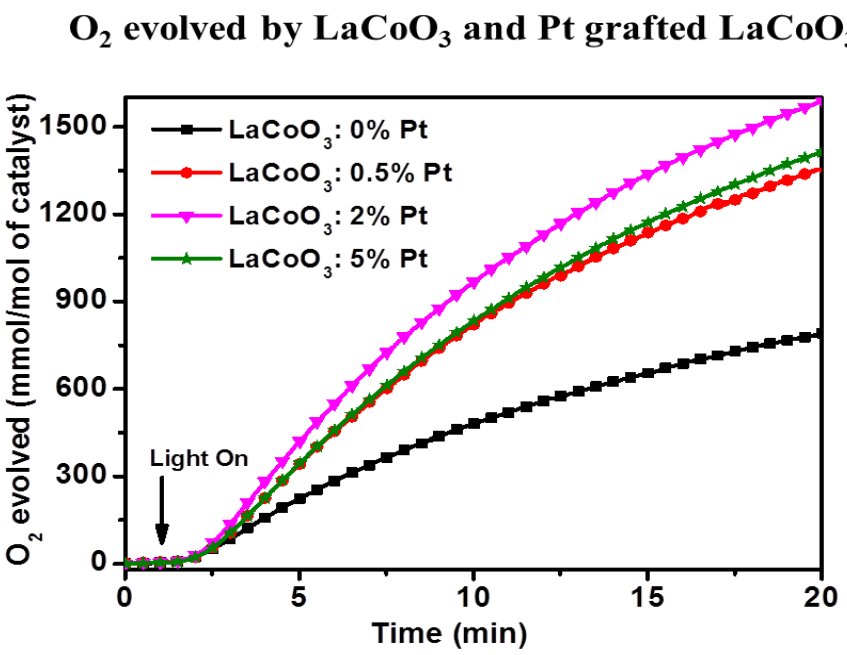

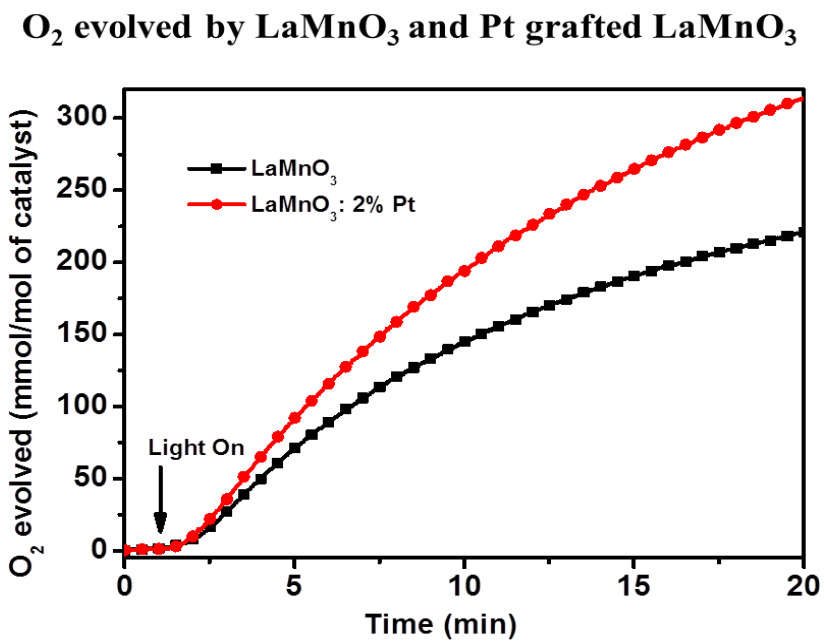

- ***Both $LaCoO_3$ and $LaMnO_3$ shows increase in activity with Pt loading.***
- ***$LaCoO_3$:Pt (2 wt%) shows twice the activity compared to $LaCoO_3$ (O_2 evolved per mole of Co) after 20 min.***
- ***$LaMnO_3$:Pt (2 wt%) shows 1.5 times the activity compared to $LaMnO_3$ (O_2 evolved per mole of Mn) after 20 min.***

Uttam Gupta, B. S. Naidu and C. N. R. Rao , **Dalton Trans.** 2015, **44**, 472-474.

Water Splitting with Semiconductors

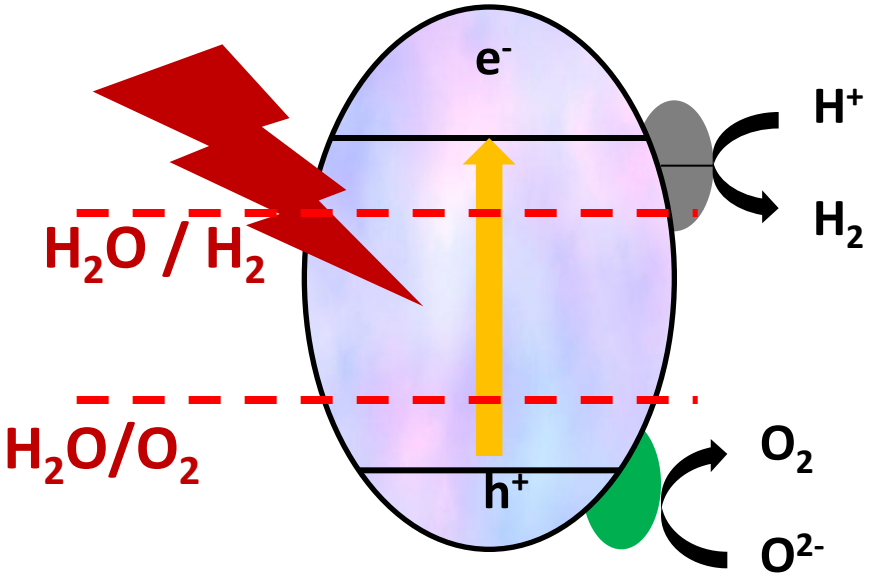

i. *Absorption of light by semiconductor*

ii. *Separation of photo-generated electron and hole pair*

iii. *Redox reactions at co-catalysts on the semiconductor*

i. *band gap > 1.23 eV (=1100 nm)*

ii. *CB more –ve than reduction potential of H^+/H_2 (0 V vs SHE)*

iii. *VB more +ve than oxidation potential of O_2/H_2O (1.23 V vs SHE)*

Some semiconductors for water splitting

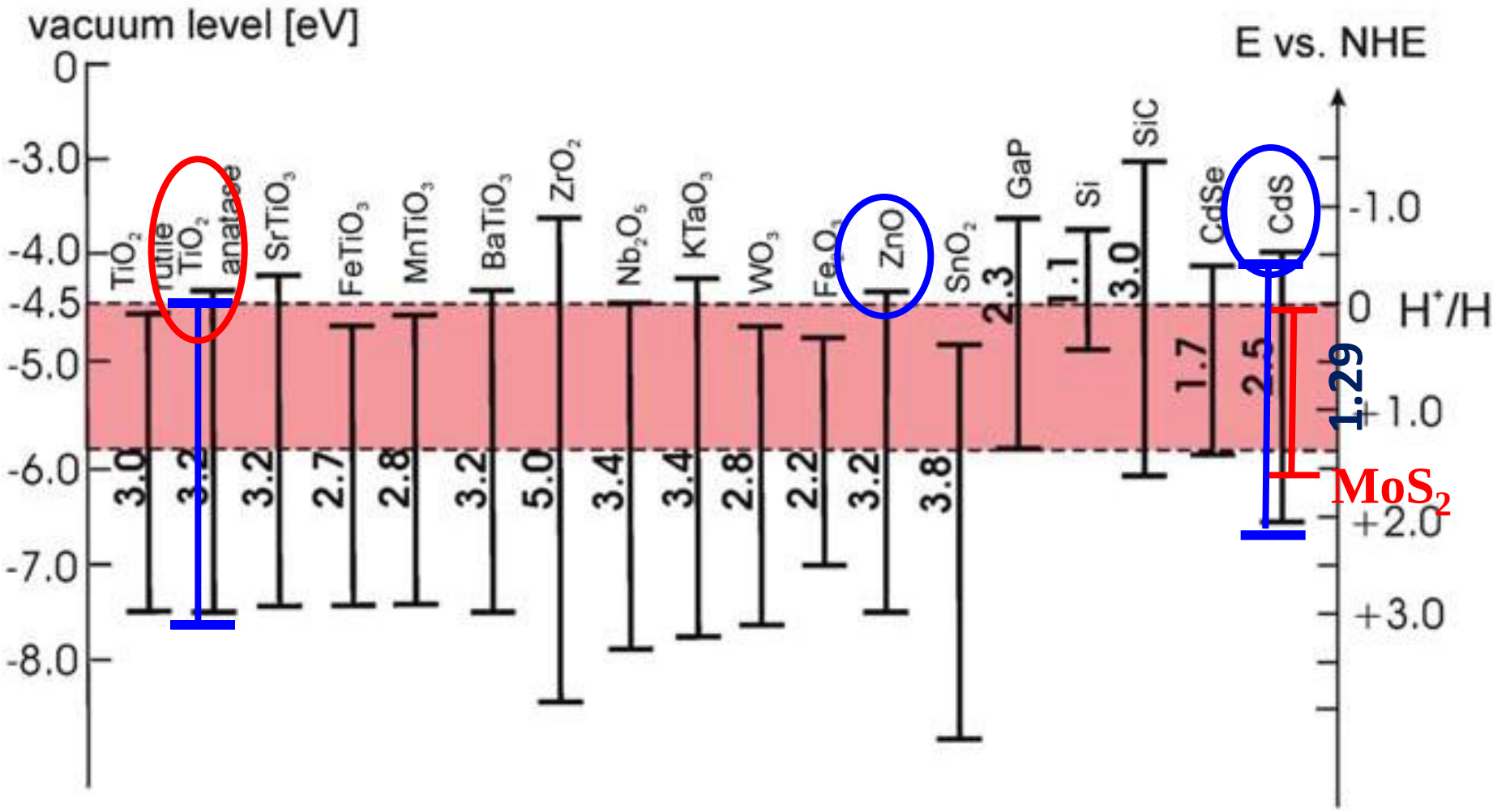

Batzill, Enery Environ. Sci, 4 (2011) 3275

Heterostructures

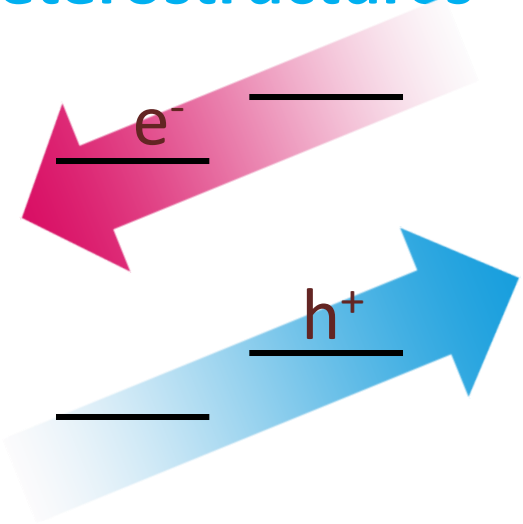

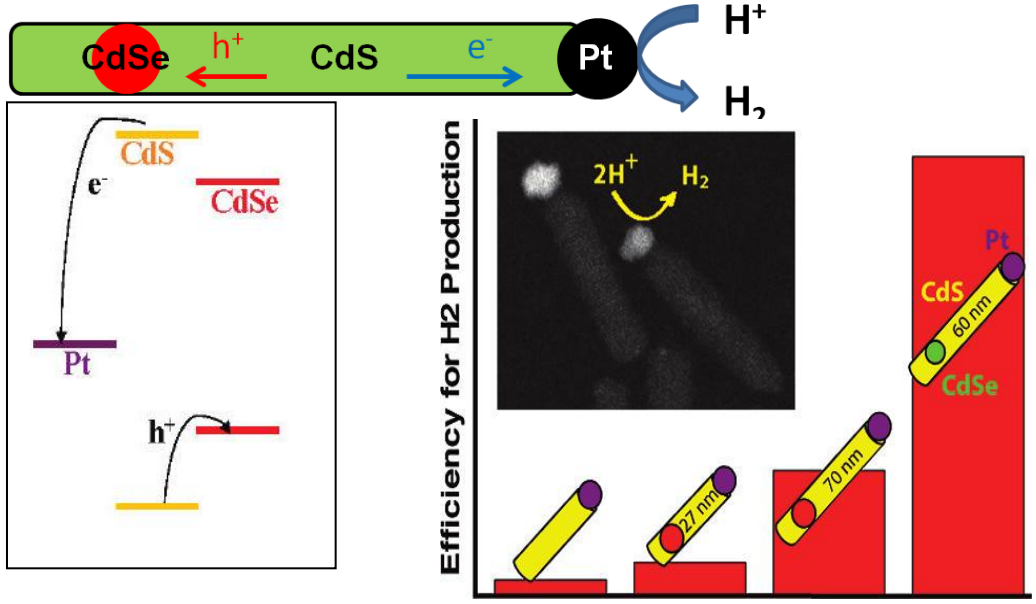

Z-Scheme

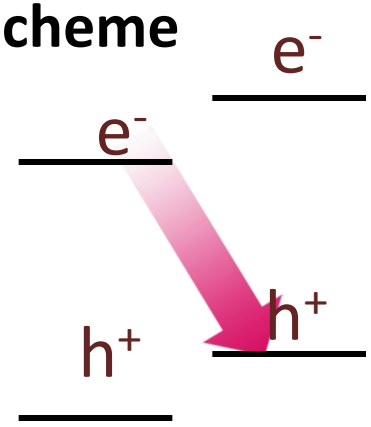

- Spatial separation of charges
- Reduced recombination of e^- and h^+

Alivisatos and co-workers J. Phys. Chem. Lett**. 2010**, 1, 1051–1054

Schemes of Photocatalytic Hydrogen Production

I) Use of Na_2S and Na_2SO_3 as sacrificial agents

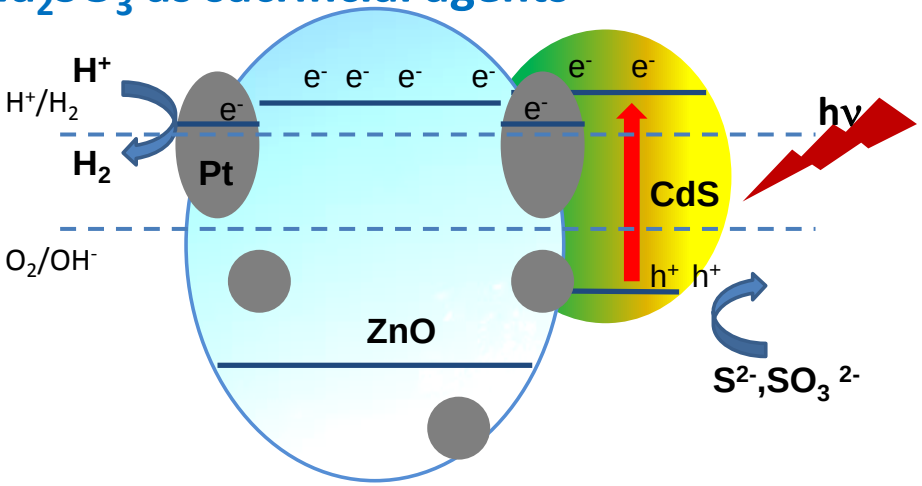

II) Use of Benzyl alcohol as sacrificial agent

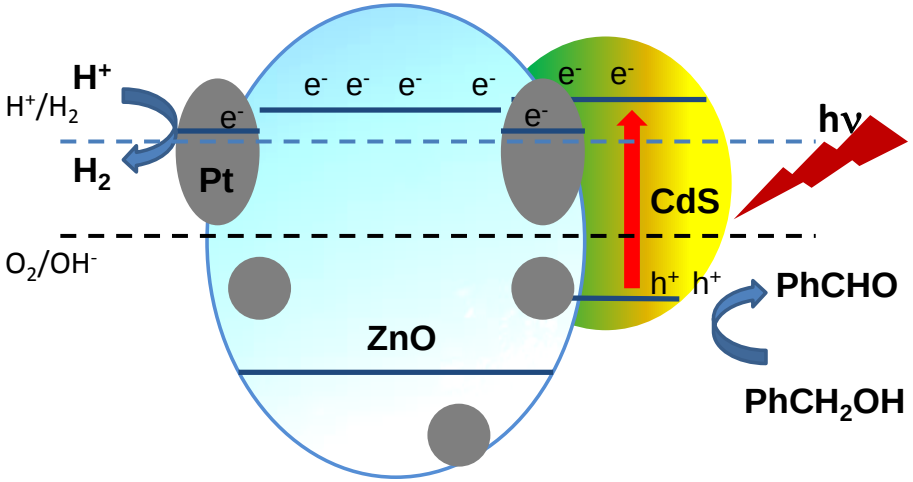

H_2 evolution and benzyl alcohol oxidation

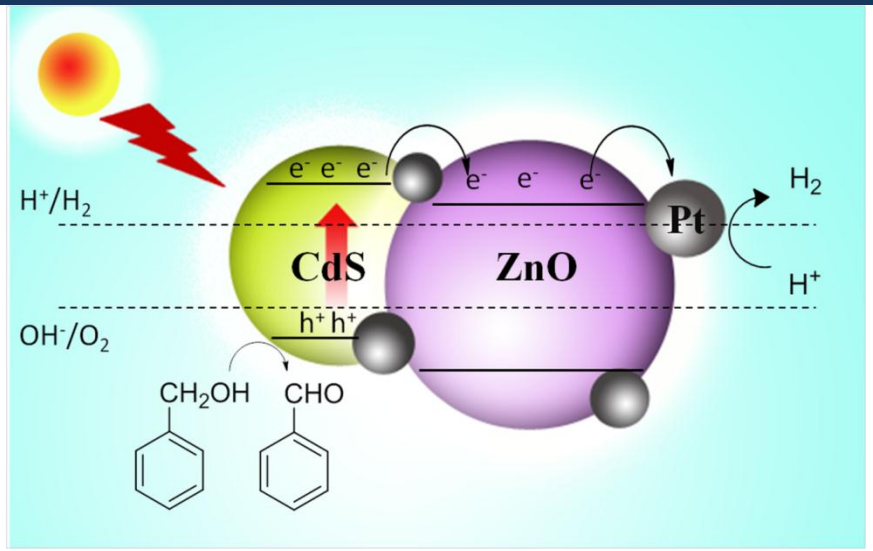

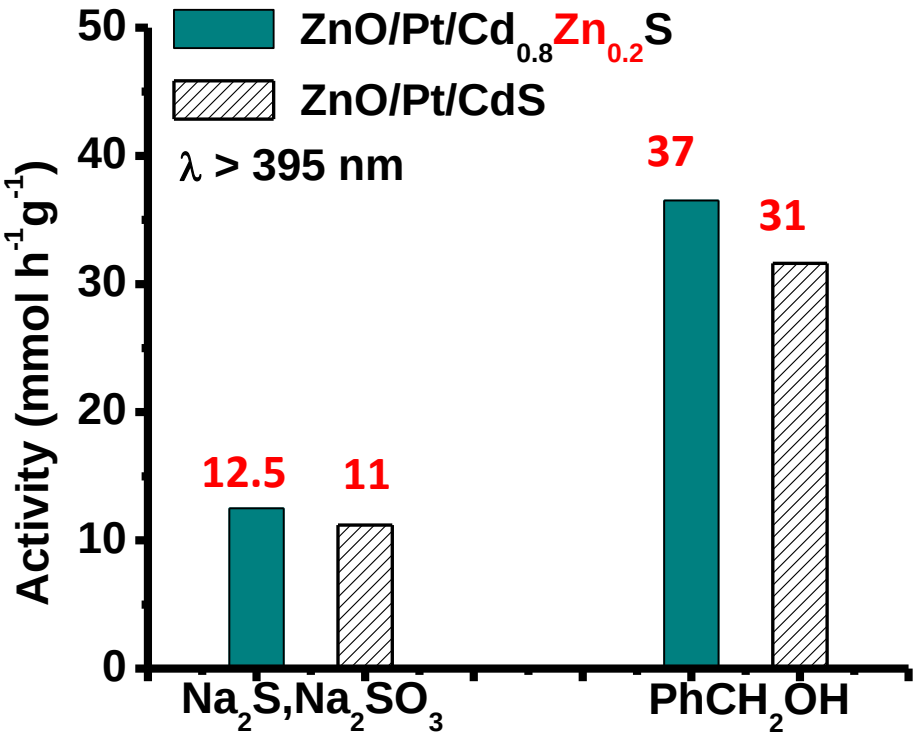

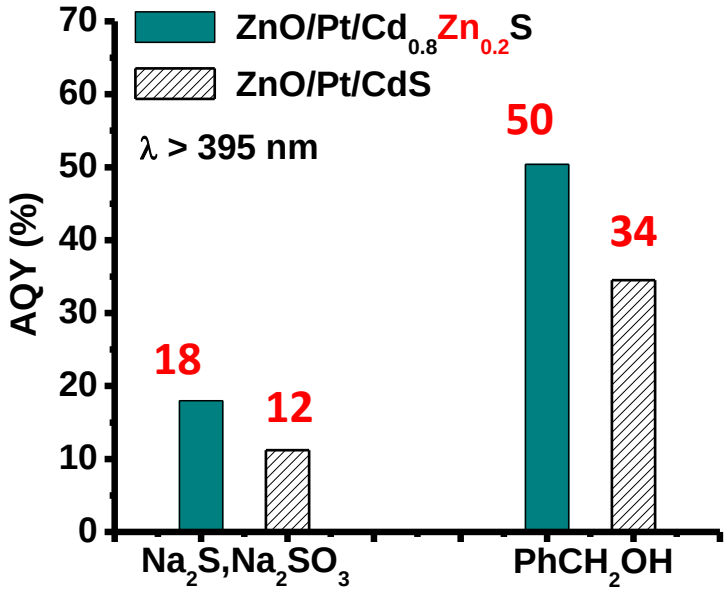

GC-MS Data:

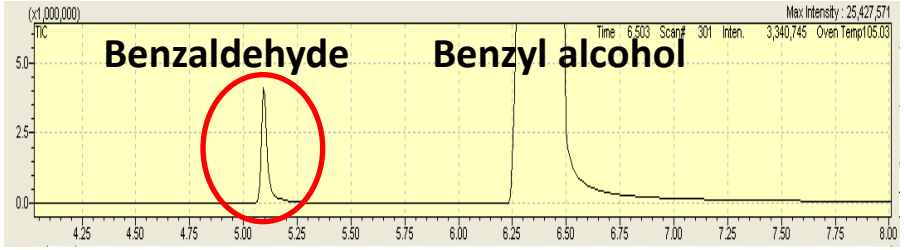

Comparison of present results with literature values of similar systems

Photocatalyst	Activity ($mmolh^{-1}g^{-1}$)	AQY (%)	Reference
ZnO/Pt/CdS[a]	**11.2[c] (17.4[d])**	**11.9[c] (11.1[d])**	**Present work**
ZnO/Pt/CdS[b]	**31.6[c]**	**34.5[c]**	**Present work**
ZnO/Pt/$Cd_{0.8}Zn_{0.2}S$[a]	**12.5[c] (31.2[d])**	**18.0[c] (23.1[d])**	**Present work**
ZnO/Pt/ $Cd_{0.8}Zn_{0.2}S$[b]	**36.5[c]**	**50.4[c]**	**Present work**
ZnO/Pt/$CdS_{0.5}Se_{0.5}$[a]	**16.0[c] (19.0[d])**	**9.3[c] (8.1[d])**	**Present work**
CdS-CdSe-Pt	**40[c]**	**20[c]**	L. Amirav, A. P. Alivisatos, *J. Phys. Chem. Lett.* **2010**, *1*, 1051.
CdS/Pt	4.4[c]	13.9[c]	Y. Li, Y. Hu, S. Peng, G. Lu, S. Li, *J. Phys. Chem. C* **2009**, *113*, 9352.
RGO-$Zn_xCd_{1-x}S$	1.8[d]	23.4[c]	J. Zhang, J. Yu, M. Jaroniec, J. R. Gong, *Nano Lett.* **2012**, *12*, 4584.
CdS-Pt	24[c]	51[c,e]	J. Yu, Y. Yu, B. Cheng, *RSC Advances* **2012**, *2*, 11829.
CdS/Pt/TiO_2	14.7[c]	13.9[c,e]	L. Qi, J. Yu, M. Jaroniec, *Phys. Chem. Chem. Phys.* **2011**, *13*, 8915.
CdS-Graphene-Pt	56[c]	22.5[c,e]	Q. Li, B. Guo, J. Yu, J. Ran, B. Zhang, H. Yan, J. R. Gong, *J. Am. Chem. Soc.* **2011**, *133*, 10878.
CdS/(Pt-TiO_2)	9[c]	4.5[c]	H. Park, W. Choi, M. R. Hoffmann, *J. Mater. Chem.* **2008**, *18*, 2379.
$Zn_xCd_{1-x}S$	11[c]	30.4[c]	Y. Wang, J. Wu, J. Zheng, R. Xu, *Catal. Sci. Technol.* **2011**, *1*, 940.
ZnO/CdS/Pt	3.9[d]	3.2[d]	X. Wang, G. Liu, Z.-G. Chen, F. Li, L. Wang, G. Q. Lu, H.-M. Cheng, *Chem. Commun.* **2009**, *0*, 3452.
CdS-$Zn_{1-x}Cd_xS$	3[c]	6.3[c]	J. Yu, J. Zhang, M. Jaroniec, *Green Chem.* **2010**, *12*, 1611.

[a] Na_2S and Na_2SO_3 are used as hole scavengers. [b] Benzyl alcohol is used as hole scavenger. [c] Visible radiation. [d] UV-visible radiation. [e] Light sources for reaction and AQY calculations are different.

Conclusions

- The ZnO/Pt/CdS nanostructures were prepared by a simple solution process.
  ZnO/Pt/CdS nanostructures exhibited a good H_2 evolution properties.

- ZnO/Pt/$Cd_{0.8}Zn_{0.2}S$ and ZnO/Pt/$CdS_{0.5}Se_{0.5}$ nanostructures were also prepared by a simple solution process.
  These nanostructures exhibited improved H_2 evolution properties.

- The use of organic molecule such as benzyl alcohol shows excellent results in H_2 evolution in addition to oxidation products such as benzaldehyde.

S. R. Lingampalli, Ujjal K. Gautam and C. N. R. Rao, *Energy Environ. Sci.*, 2013, 6, 3589–3594.

$ZnO_{1-x}(N,F)_x/Pt/Cd_{1-y}Zn_yS$ nanoheterostructures

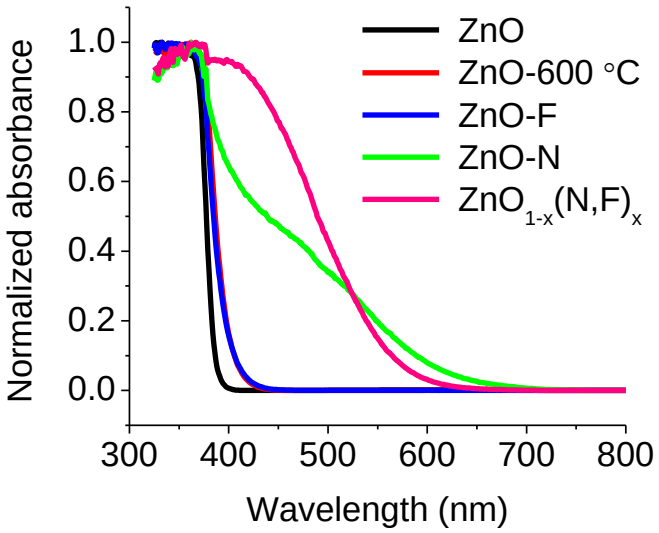

$$ZnO \xrightarrow[\Delta]{NH_3,\ NH_4F} ZnO_{1-x}(N,F)_x$$

C. N. R. Rao and co-workers, ChemPhysChem 2013, 14, 2672 – 2677

- Atomic content of **N 18 %** and **F 20 %**
- Absorption spectrum extended to visible light due to band structure modifications

Formation of heterostructures with visible light sensitive ZnO and CdS is an interesting strategy for the visible light induced hydrogen evolution.

TEM Image of $ZnO_{1-x}(N,F)_x/Pt/CdS$

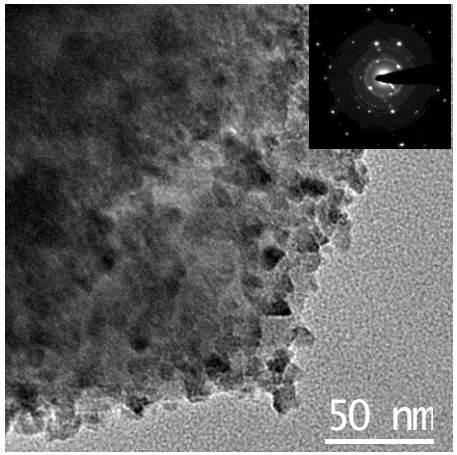

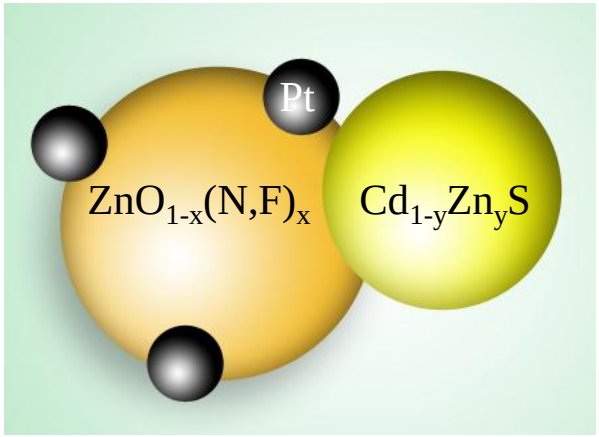

Comparison of hydrogen evolution studies on ZnO/Pt/CdS and ZnO(N,F)/Pt/CdS

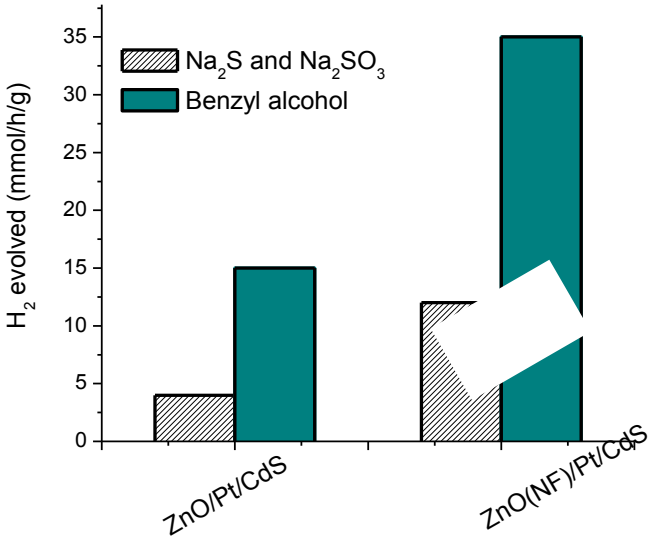

ZnO(N)/Pt/CdS and ZnO(N,F)/Pt/CdS have shown excellent hydrogen evolution with a rate of 35 mmol/h/g with and AQY of 30 % in the presence of benzyl alcohol as sacrificial agent under visible light irradiation.

Effect of substitution of Zn as in $ZnO_{1-x}(NF)_x/Pt/Cd_{0.8}Zn_{0.2}S$

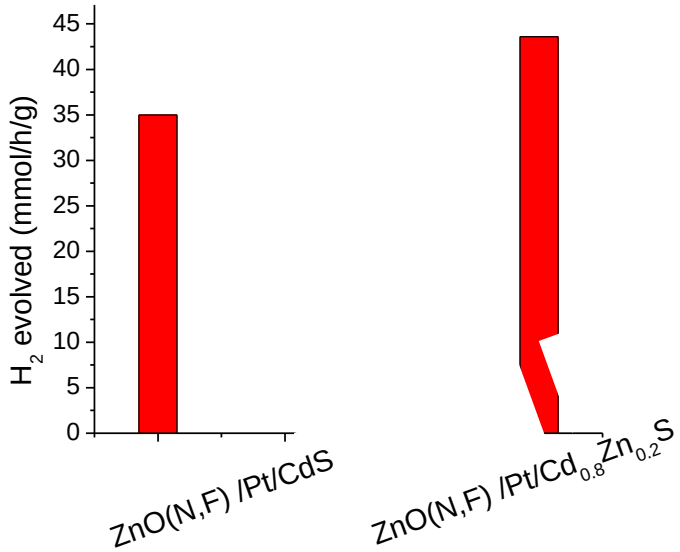

Substitution of Zn in CdS has further improved the hydrogen evolution with an evolution rate of 43 mmol/h/g (AQY 44 %).

S. R. Lingampalli and C. N. R. Rao, J. Mater. Chem. A 2014, 2, 7702–7705.

H_2 evolution by N,F codoped TiO_2

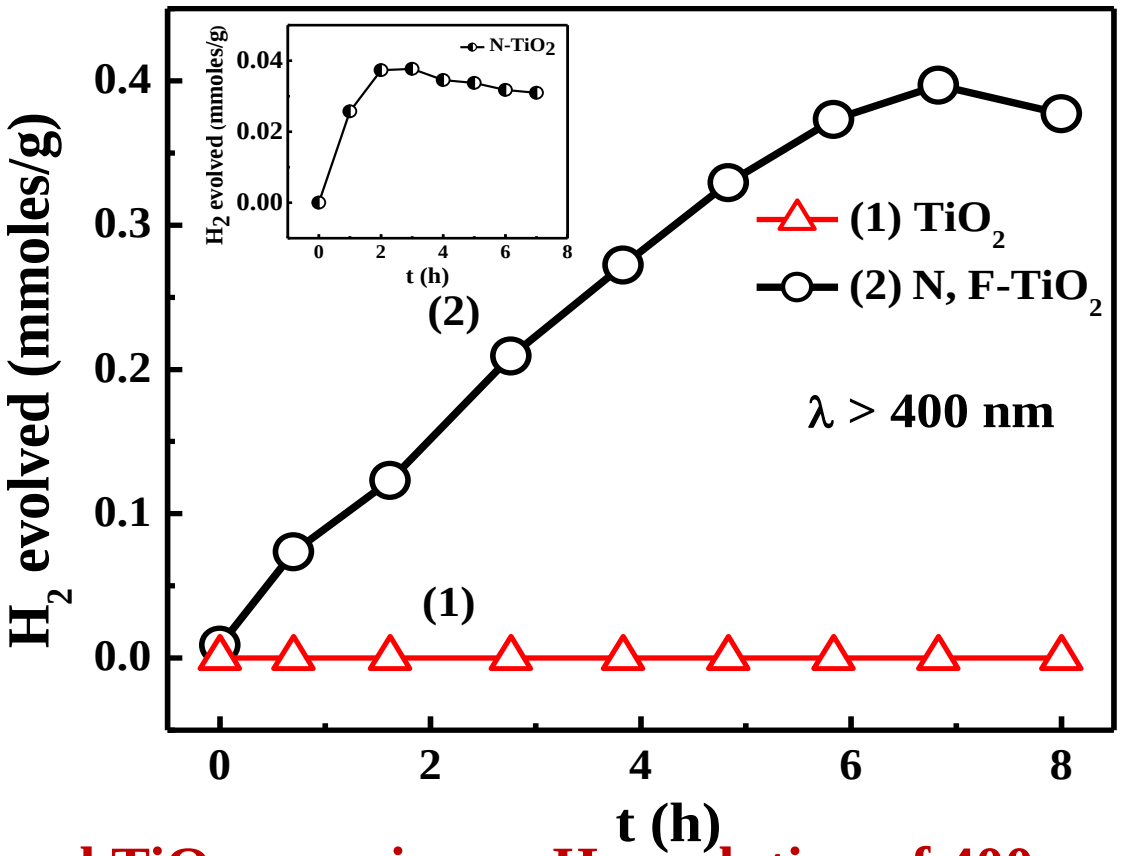

N, F co-doped TiO_2 - maximum H_2 evolution of 400 μmoles/g rate of ~ 60 μmoles/g/h without the loading of any noble metal or other co-catalyst.

N-doped TiO_2 - 37 μmoles/g

N.Kumar, U. Maitra, V. I. Hegde, U. V. Waghmare, A. Sundaresan, C. N. R. Rao, Inorg. Chem. 2013, 52, 10512−10519.

Use of NiO as a co-catalyst in ZnO/NiO/CdS type heterostructures

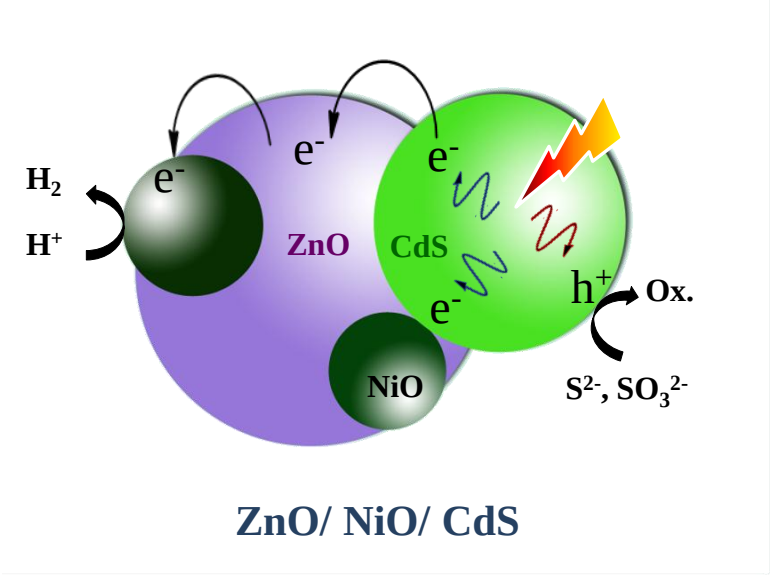

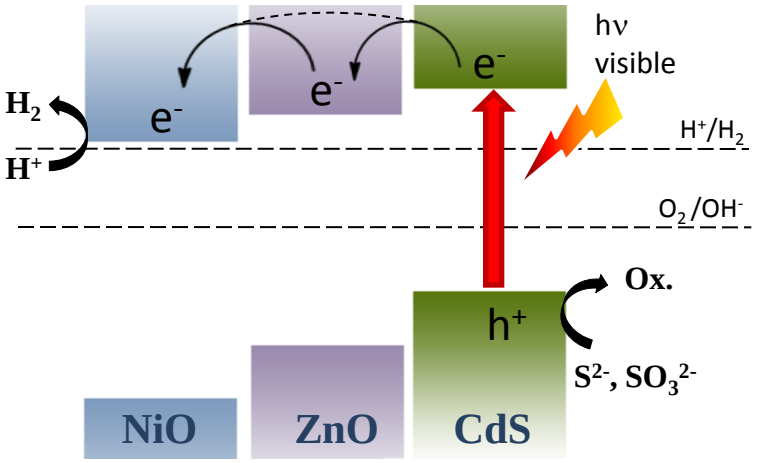

Vectorial ordering of conduction band minimum in this system allows efficient charge-separation and the reduction of proton to hydrogen.

Advantages

- Noble-metal free
- Highly efficient
- Easy to synthesize

Comparison of H_2 evolution activities

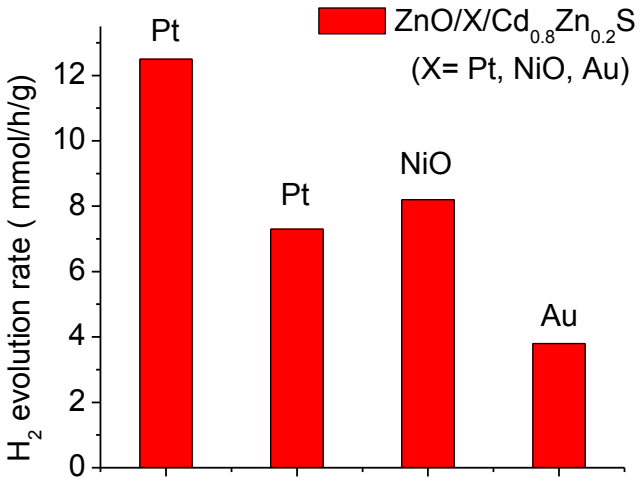

- $ZnO/NiO/Cd_{1-x}Zn_xS$ (x=0.0, 0.2) heterostructures are highly active under visible as well as UV-visible irradiation.
- Activities of $ZnO/NiO/Cd_{1-x}Zn_xS$ (x=0.0, 0.2) are comparable or superior to those obtained with Pt and Au co-catalysts.
- Activities and quantum yields of $ZnO/NiO/Cd_{1-x}Zn_xS$ (x=0.0, 0.2) are superior to many of the literature reports using NiO as a co-catalysts.

S. R. Lingampalli, A. Roy, M. Ikram and C. N. R. Rao, **Chem. Phys. Lett.** 2014, **610,** 316-320.

H_2 evolution on $(TiO_2)_{1-x}(NiO)_x/Cd_{0.8}Zn_{0.2}S$ (x =0-1)heterostructures

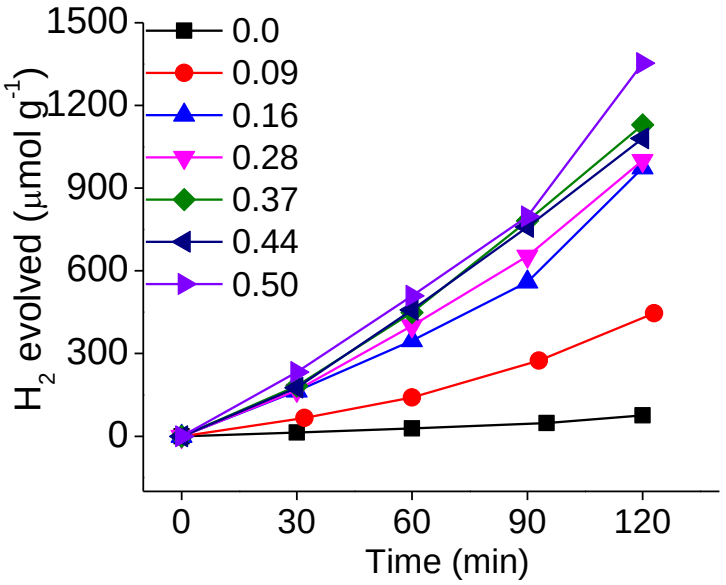

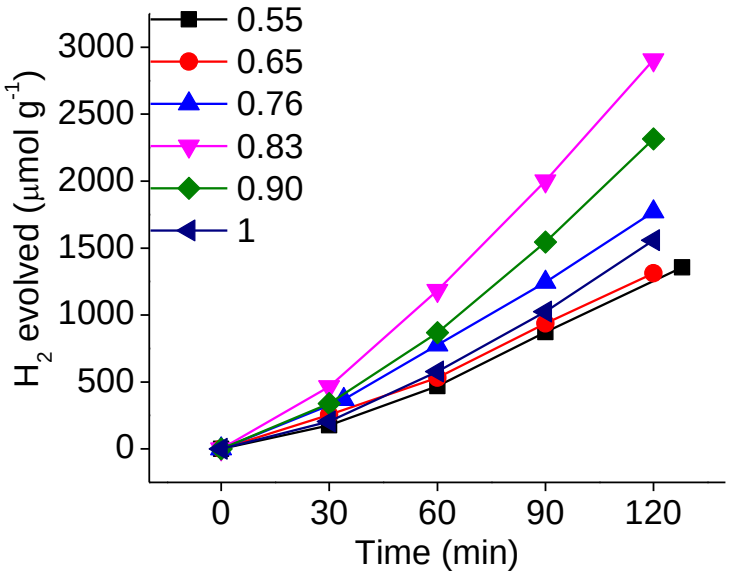

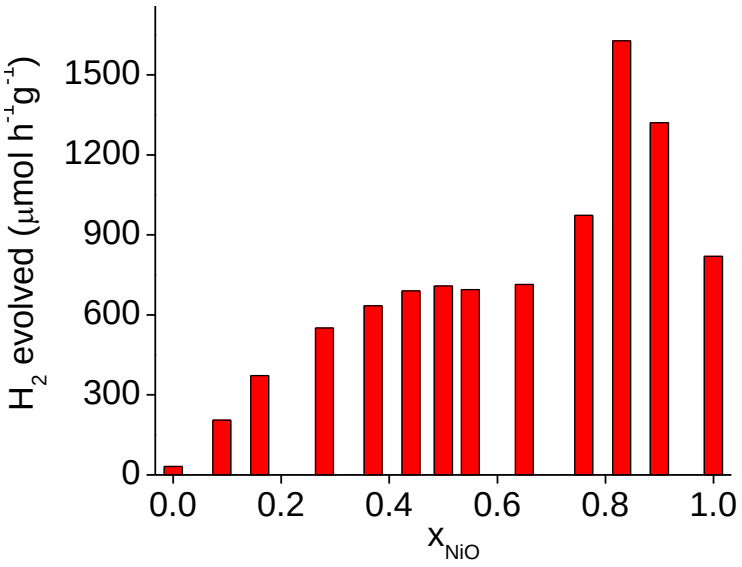

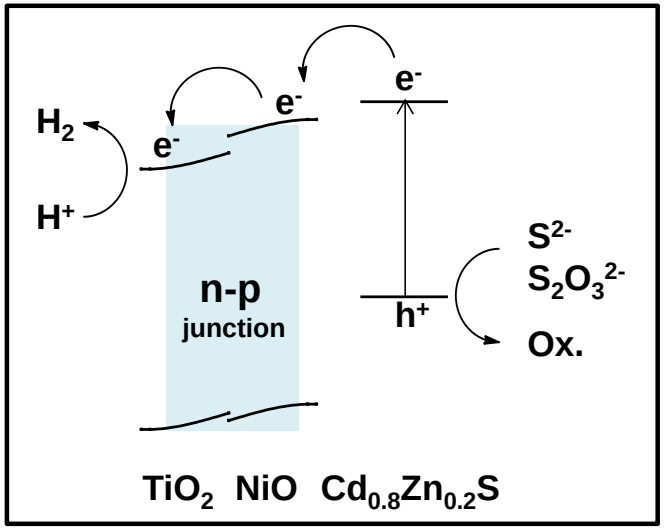

A. Roy, S. R. Lingampalli and C. N. R. Rao, **Chem. Phys. Lett**. 2015, **637,** 137-142.

MoS_2 for Photocatalytic H_2 evolution

Colloidal MoS_2 nanoparticles

- *$[Ru(bpy)_3]^{2+}$ sensitized*
- *TON of 93*

Chem. Comm. 2009, 0, 4536

RGO-MoS_2 composite

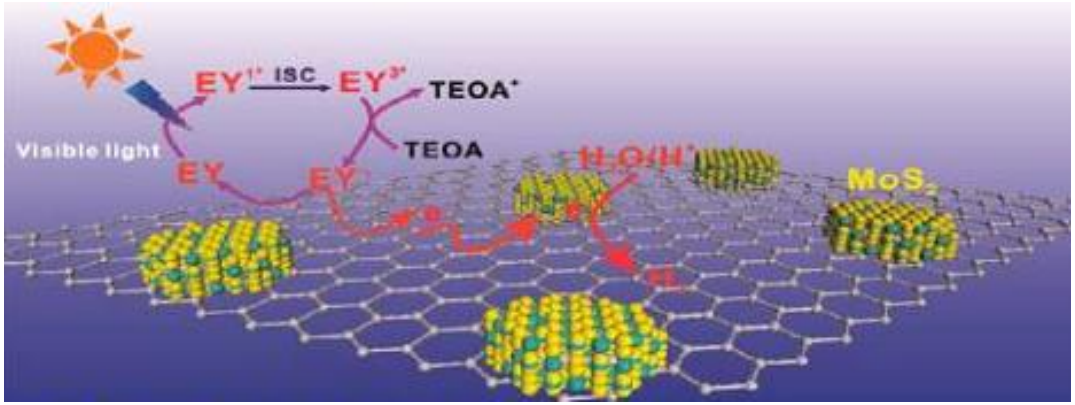

- *Eosin Y sensitized*
- *Yeild 2 mmoles.g^{-1}.h^{-1}*

J Phys. Chem. C 2012, 116, 25415

Mechanism of H_2 evolution in Graphene-MoS_2 composites

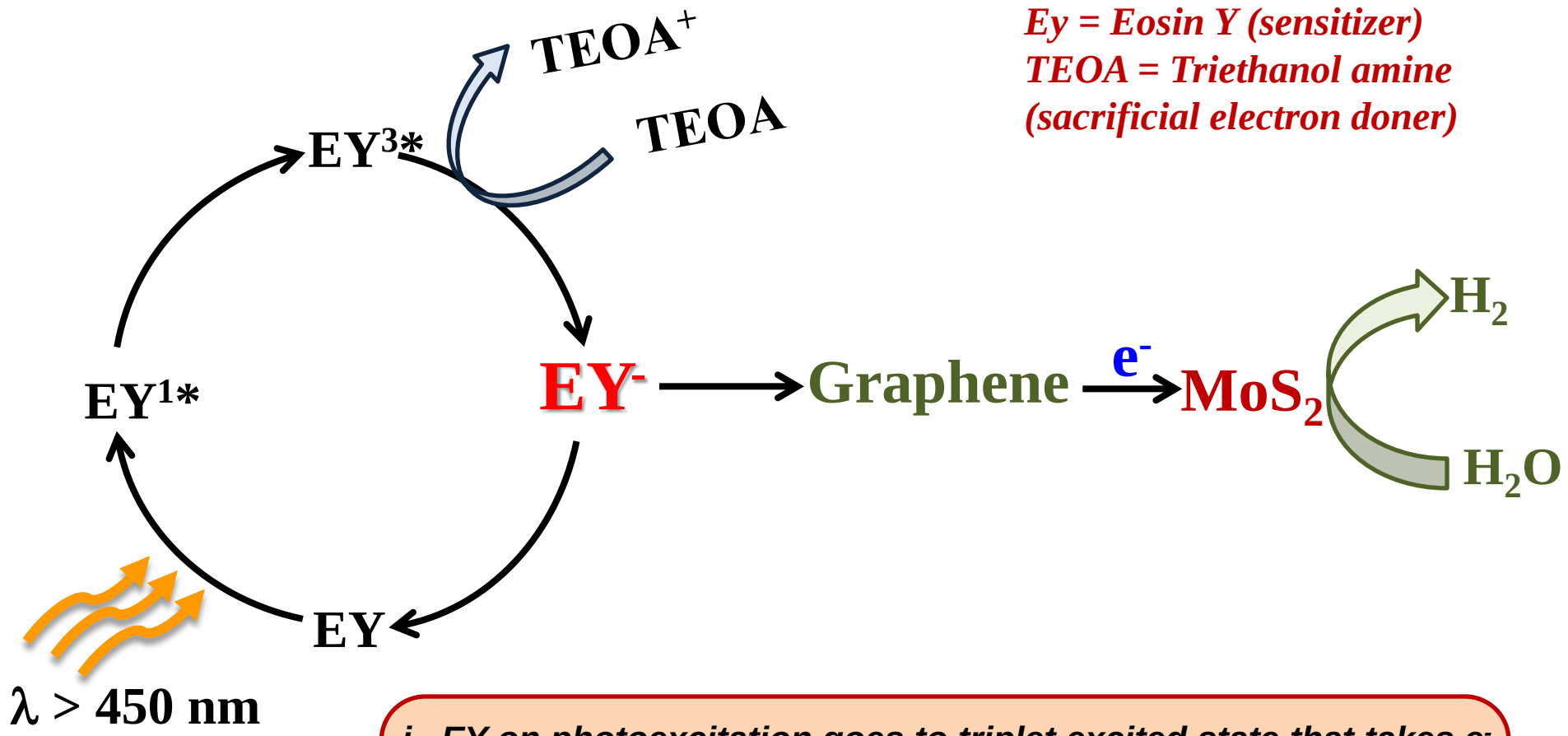

Ey = Eosin Y (sensitizer)
TEOA = Triethanol amine (sacrificial electron doner)

i. EY on photoexcitation goes to triplet excited state that takes e^- from TEOA and forms EY anion

ii. EY^- being highly reactive donates an e^- to Graphene which then transfers this e^- to MoS_2 for water reduction

Urmimala Maitra, Uttam Gupta, Mrinmoy De, Ranjan Datta, A. Govindaraj, and C. N. R. Rao, Angew. Chem. Int. Ed.2013, 52, 13057.*

Photocatalytic H_2 evolution by MoS_2- graphene composites

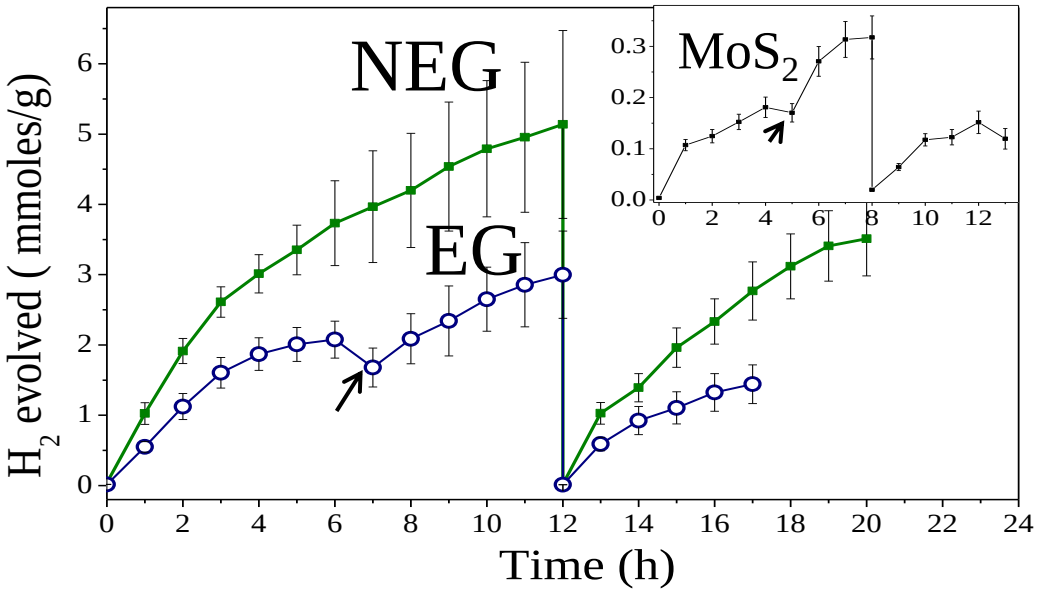

Sample	Yield/h (mmoles $g^{-1}h^{-1}$)	TOF (h^{-1})
MoS_2	**0.05**	**0.008**
EG-MoS_2	**0.54**	**0.21**
NEG-MoS_2	**0.83**	**0.45**

NEG = 5% N doped graphene

NEG-MoS_2> EG-MoS_2 > MoS_2

**** MoS_2 prepared at high temperature.***

- ***Graphene acting as electron channel.***
- ***N doped (electron rich) favors electron transfer from graphene to MoS_2***

Photocatalytic H_2 evolution by MoS_2- graphene composites

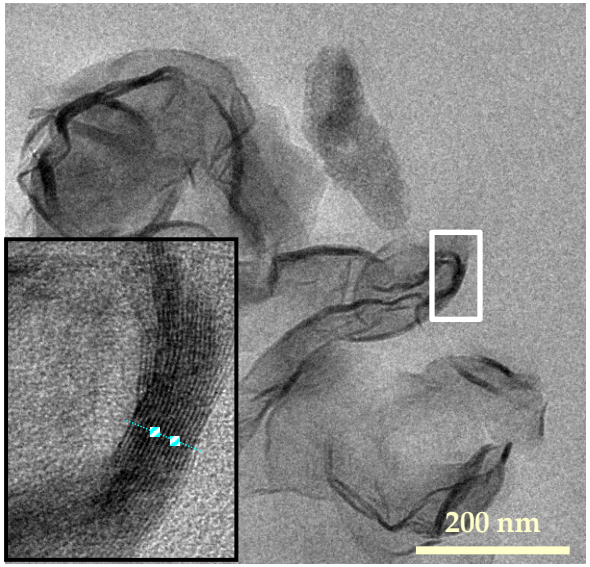

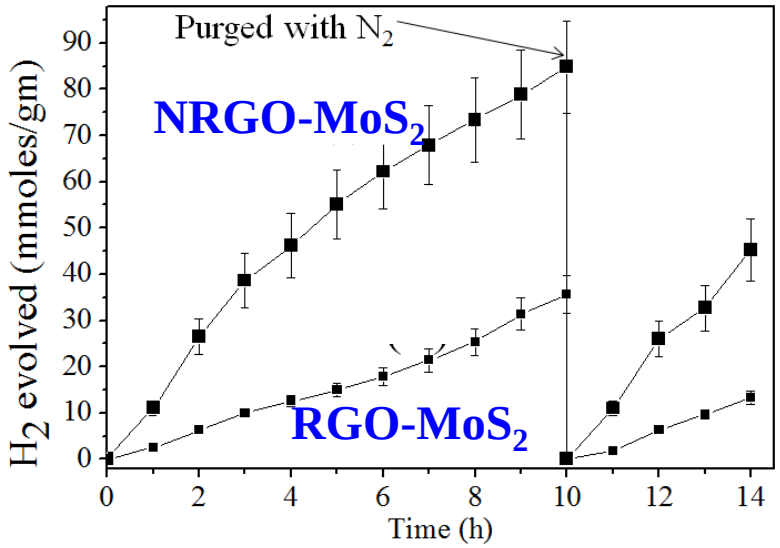

NRGO= Highly N doped RGO ~ 15 atomic %

NRGO-MoS_2> RGO-MoS_2 >> MoS_2

- ***NRGO is highly e^- rich and thus transfers e^- easily to MoS_2***
- ***Greater stacking of MoS_2 thus higher density of edges***
- ***MoS_2 grows perpendicular to NRGO (the electron donating substrate) thus better electron transfer.***

Sample	Yield/h (mmoles $g^{-1}h^{-1}$)	TOF (h^{-1})
MoS_2	**0.05**	**0.008**
RGO-MoS_2	**3**	**0.68**
NRGO-MoS_2	**10.8** **42(400W)**	**2.9** **11.5(400W)**

Chemically exfoliated MoS_2

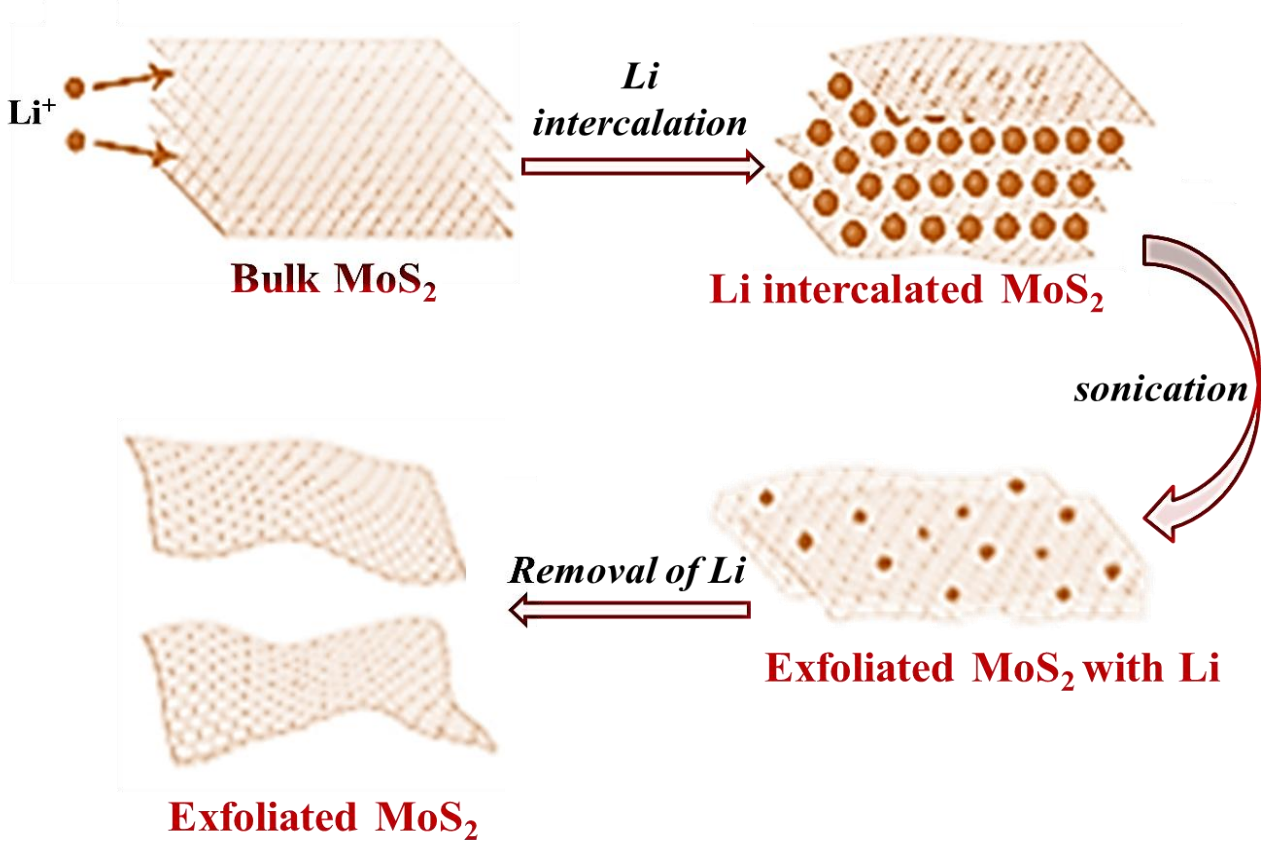

- *MoS_2 prepared by Li intercalation and exfoliation is known to exits as 1T-MoS_2 polytype*
- *1T-MoS_2 is metallic*

HRTEM and ED showing 1T state

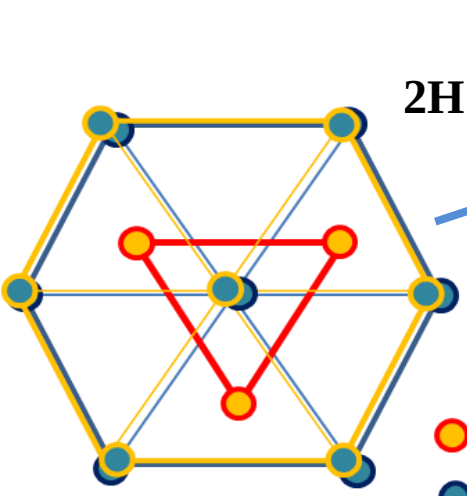

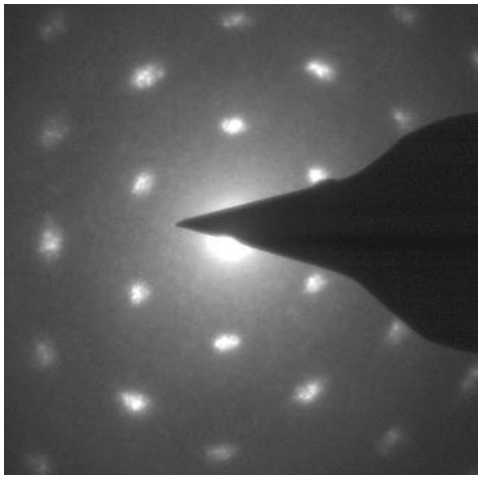

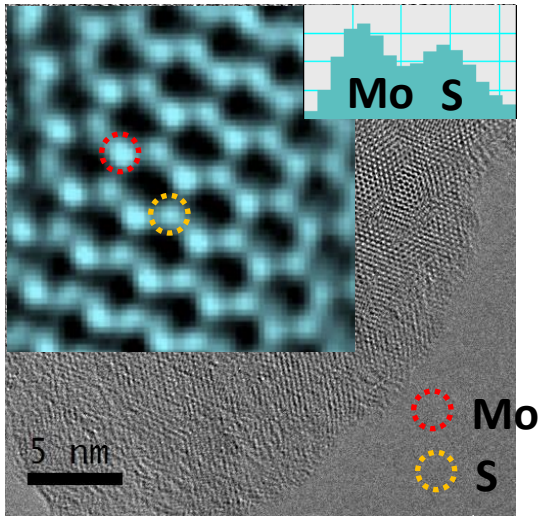

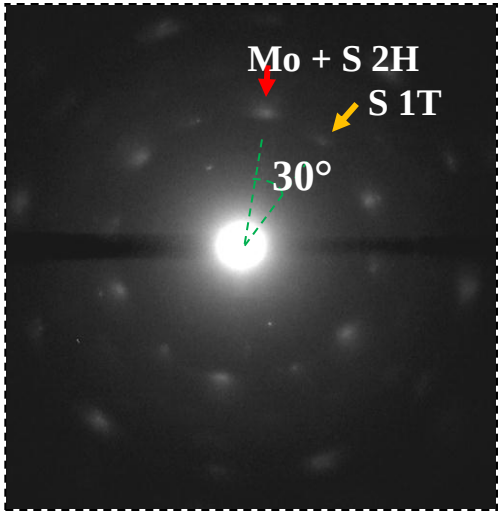

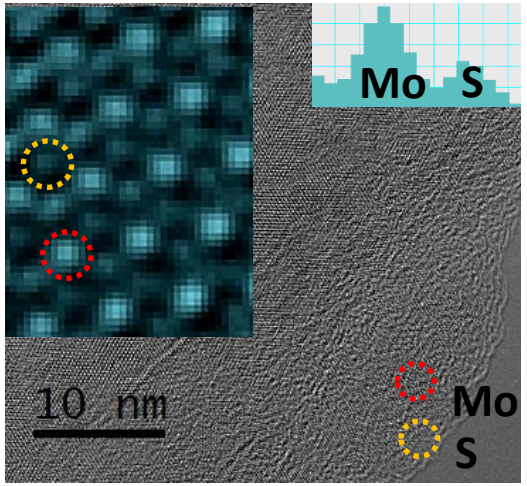

H_2 evolution by chemically exfoliated MoS_2(1T)

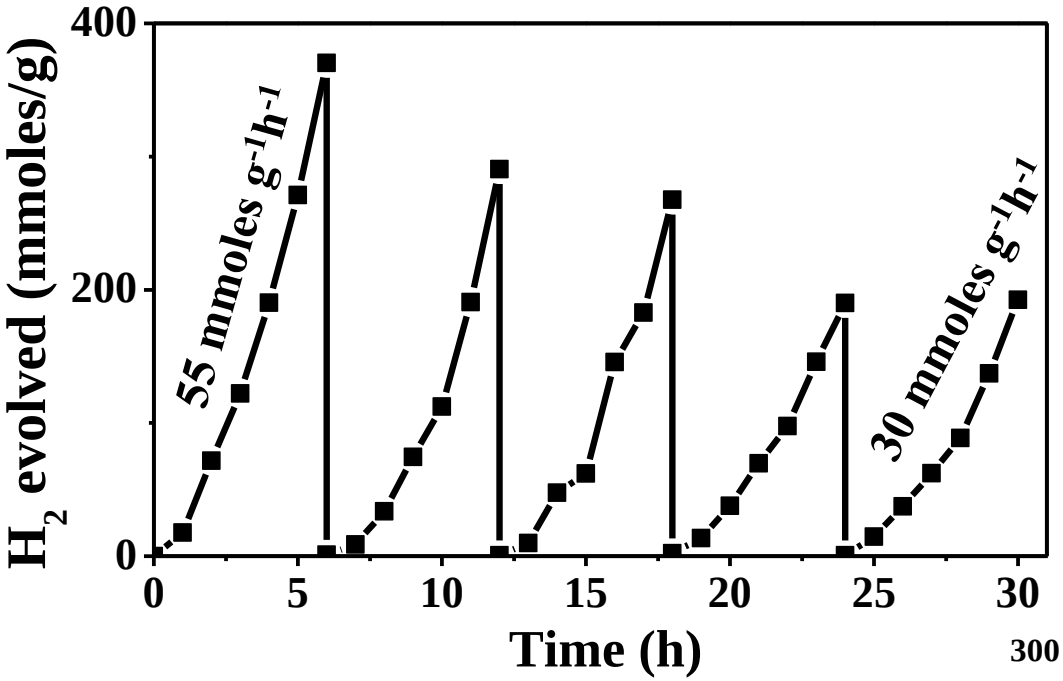

Time course of H_2 evolution by 1T-MoS_2 over a period of 30 hrs with purging after every 6 hrs

Time course of H_2 evolution by 1T-MoS_2 - as prepared dispersion & dispersion stored for 30 days.

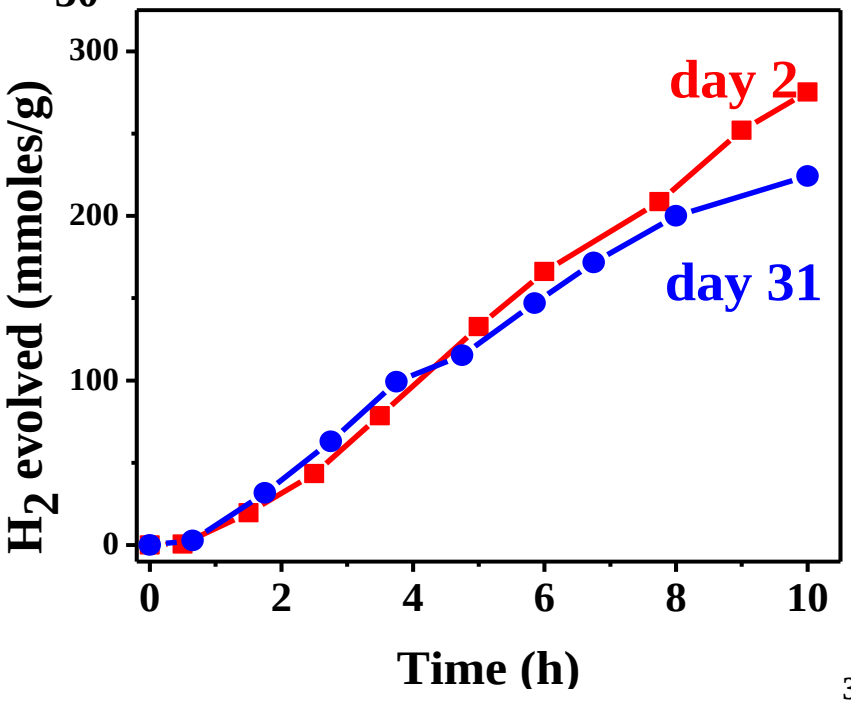

Mechanism of H_2 evolution by 1T-MoS_2

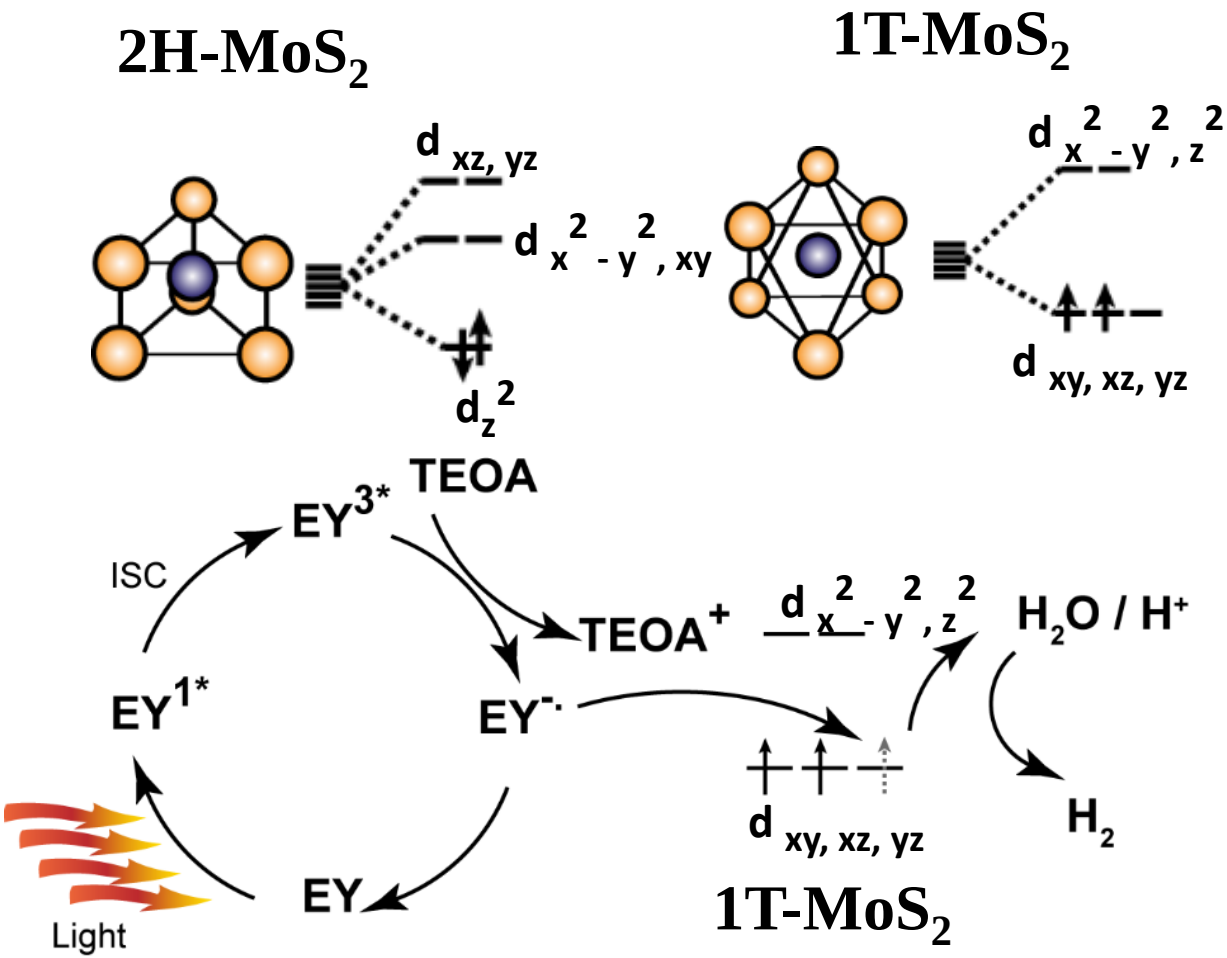

2H- MoS_2 – filled $4d_{z^2}$ and four empty doubly degenerate orbitals composed of ($4d_{xy}$, $_{x^2-y^2}$) and ($4d_{xz}$ $_{,yz}$)

1T MoS_2 - three triply degenerate orbitals $4d_{xy,\ xz,\ yz}$ containing two unpaired electron and two empty doubly degenerate orbital 4d $_{x^2-y^2,z^2}$.

- *Electron transfer directly from EY^- to empty $4d_{xy,\ xz,\ yz}$ MoS_2*
- *Presence of makes it metallic as well as highly active catalyst*

Comparison of H_2 evolution by 2H and 1T MoS_2

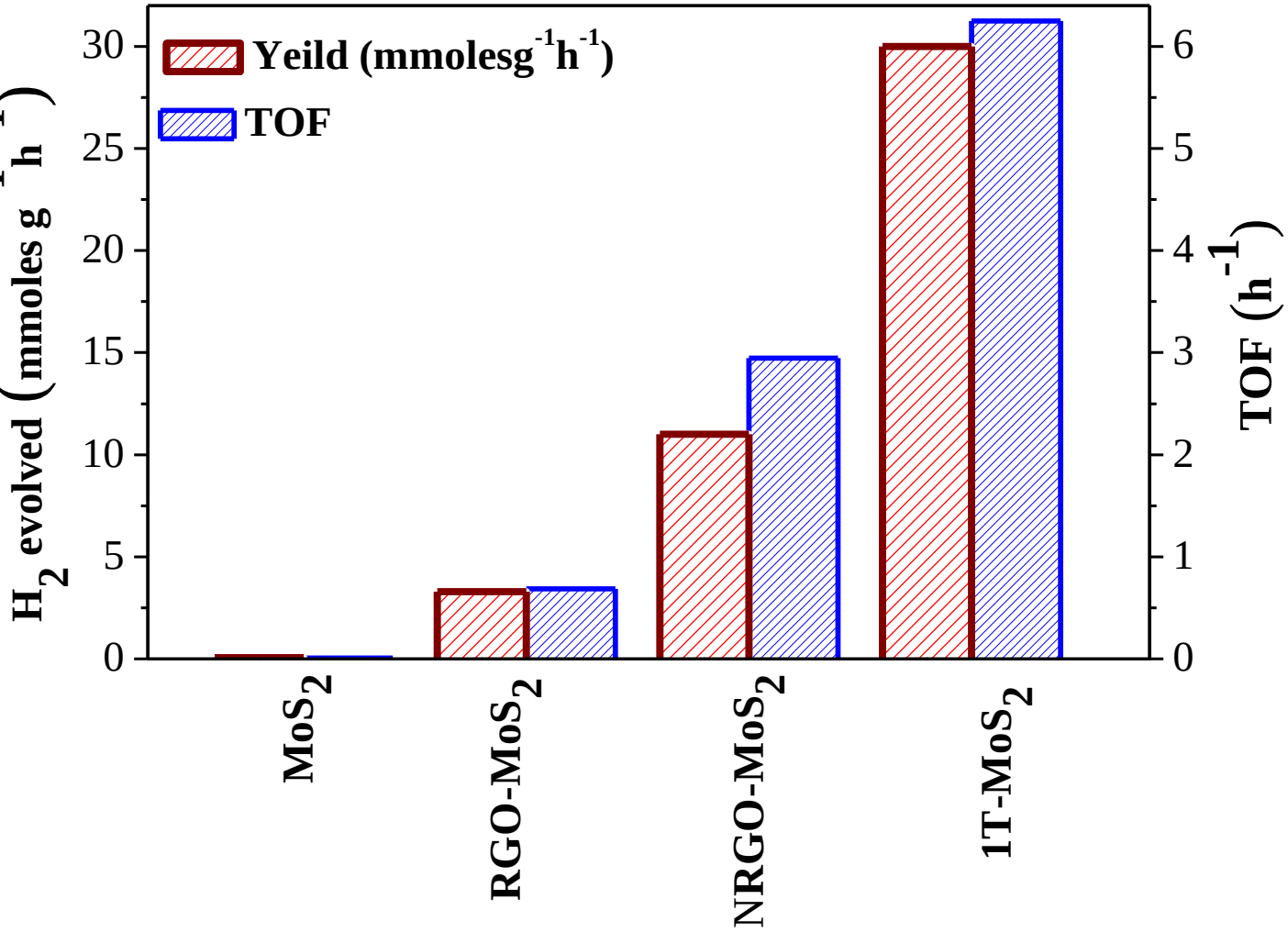

Comparison of H_2 evolution by 2H and 1T $MoSe_2$

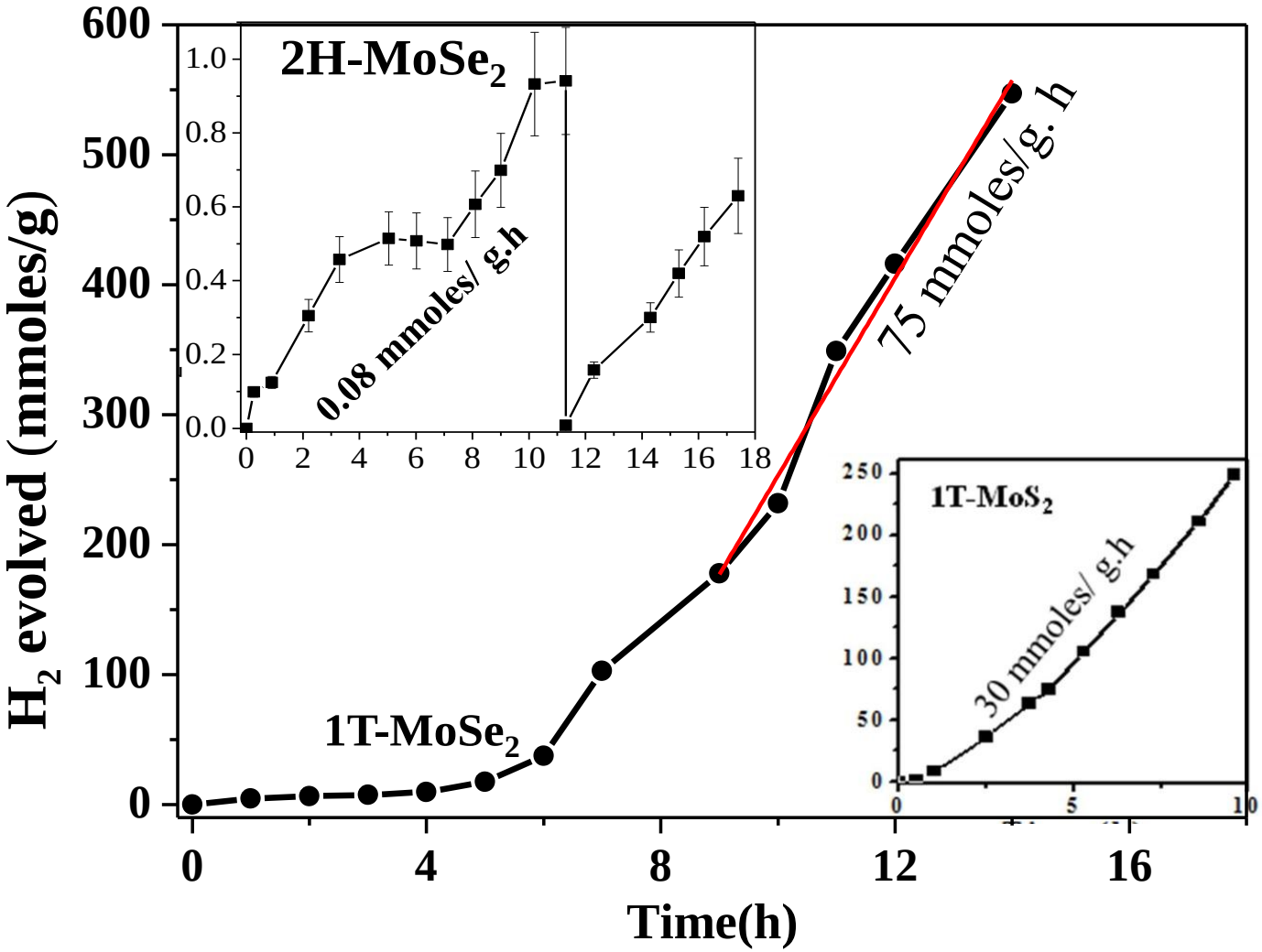

Rao et. al APL (Materials) (2014)

Hydrogen evolution activity of $MoSe_2$, MoS_2 and TaS_2 based catalysts

Compounds	Light Source	Activity ($mmol\ h^{-1}\ g^{-1}$)	TOF (h^{-1})
MoS_2/CdS	300 W Xe lamp	5.3	ca. 0.7
TaS_2/CdS	400 W Xe lamp (λ>399nm)	2.32	0.57
2H MoS_2 [a]	100 W Halogen lamp	0.05	0.008
NRGO-MoS_2 [a]	100 W Halogen lamp	10.8	2.9
1T MoS_2 [a]	100 W Halogen lamp	30	6.5
1T-$MoSe_2$ [a]	100 W Halogen lamp	70±5	19.2
Few layer 2H $MoSe_2$ [a]	100 W Halogen lamp	0.05	0.02

TOF calculated per mole of catalytically active material (Graphene is considered to be inactive compared to MoS_2). [a] Eosin Y dye sensitized

Conclusions

i. Obtained highest photocatalytic H_2 evolution rate in any MoS_2 based system reported thus far.

ii. Nanoflakes of MoS_2 with high density of catalytically active edges, grown on heavily N-doped graphene gives the best yield among all 2H-polytype of MoS_2.

iii. N-doping of graphene not only improved the electron donating ability of graphene but also created a p-n junction that suppresses charge recombination.

iv. Metallic 1T-polytype of MoS_2shows extraordinary HER activity by virtue of its metallic nature and intrinsic high catalytic activity.

v. Catalytic activity of 1T-MoS_2 is about 600-1000 times that of 2H-MoS_2.

vi. 1T-$MoSe_2$ shows extraordinarily high catalytic activity, being the best catalyst by far.

Urmimala Maitra, Uttam Gupta, Mrinmoy De, Ranjan Datta, A. Govindaraj, and C. N. R. Rao, Angew. Chem. Int. Ed.2013, 52, 13057.*

Uttam Gupta, B.S. Naidu, Urmimala Maitra, Anjali Singh, Sharmila Shirodkar, Umesh V. Waghmare and C.N.R. Rao, APL Materials , 2014.*

Thermochemical Splitting of CO_2 and H_2O

Are There Other Ways of Splitting Water?

1) by heat! (catalysis to bring down the temperature of decomposition)

2) Solar-Thermochemical route using oxides:

Basic two steps involved in high temp TCDS/TWS:

$$\text{Endothermal Step: } MO_n \rightarrow MO_{n-\delta} + {}^{\delta}/_{2}\, O_2 \text{ ------ } (1)$$

$$\text{Exothermal step: } MO_{n-\delta} + \delta CO_2 \rightarrow MO_n + \delta CO \text{ --- } (2)$$
$$MO_{n-\delta} + \delta H_2O \rightarrow MO_n + \delta H_2$$

State-of-art material

$$CeO_2 \rightarrow CeO_{2-\delta} + {}^{\delta}/_{2}\, O_2 \quad ------ (1)$$

$$CeO_{2-\delta} + \delta\, H_2O(CO_2) \rightarrow CeO_2 + \delta H_2(CO) \quad -- (2)$$

Chueh et. al. Science, **2010**, *330*, 1797

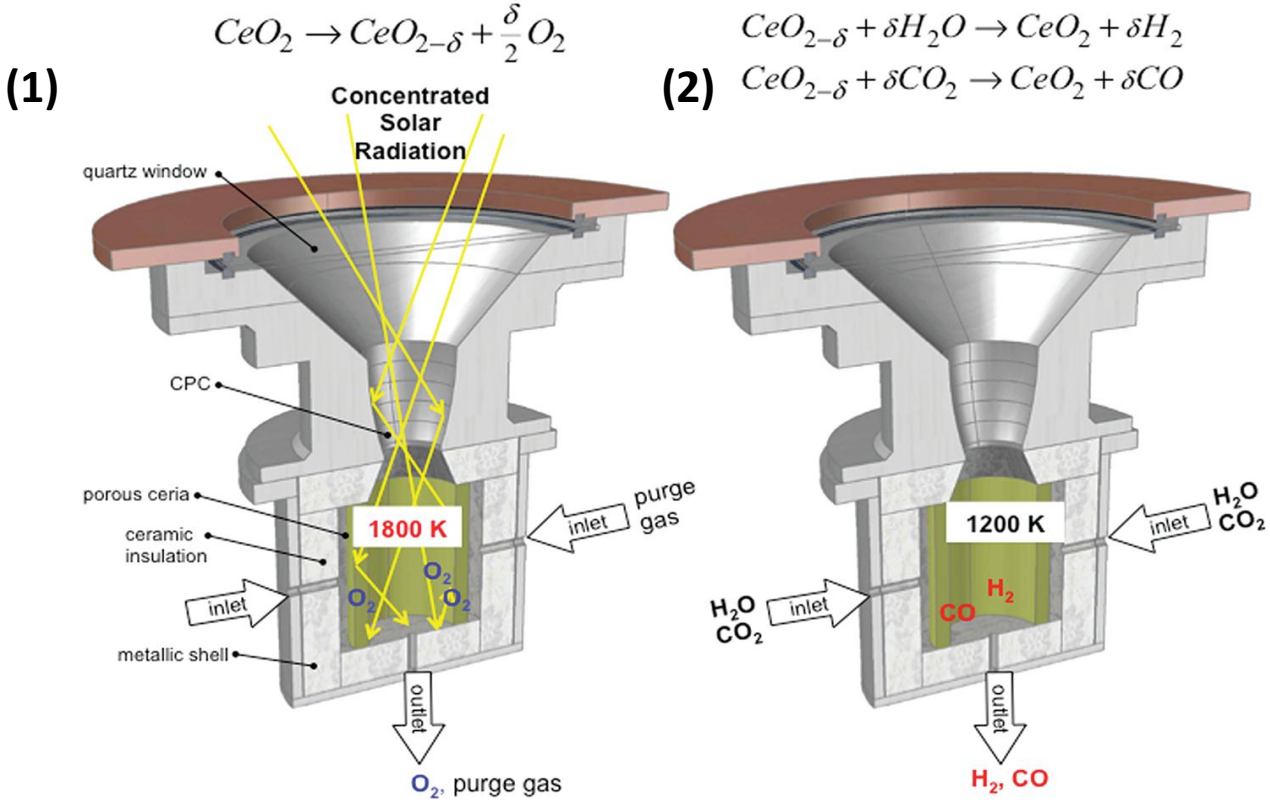

Reaction set up of **ETH's** High flux solar simulator. Solar cavity receiver containing a porous ceria cylinder that is directly exposed to high-flux solar irradiation entering through a windowed aperture. Reacting gases flow radially across the porous ceria, while product gases exit the cavity through an axial outlet port.

Perovskite oxides

$La_{1-x}Sr_xMnO_3$ is recently came into the picture & reported to show good activity than CeO_2.

Mc Daniel et.al. ***Energy Environ. Sci.***, 2013, **6**, 2424;
Yang et. al. ***J. Mater. Chem. A,*** 2014**, 2,** 13612;

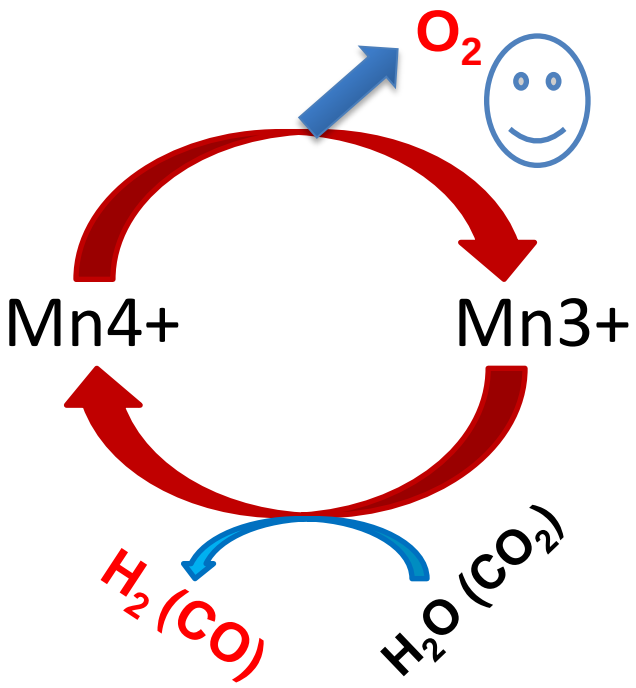

- **Sr^{2+} substitutes La $^{3+}$ and Mn^{4+} concentration increases.**
- **Reduction at 1400°C converts Mn^{4+} to Mn^{3+} ; evolves O_2.**
- **Mn^{3+} converts back to Mn^{4+} : splits H_2O and CO_2**

Noteworthy performance of $La_{1-x}Ca_xMnO_3$

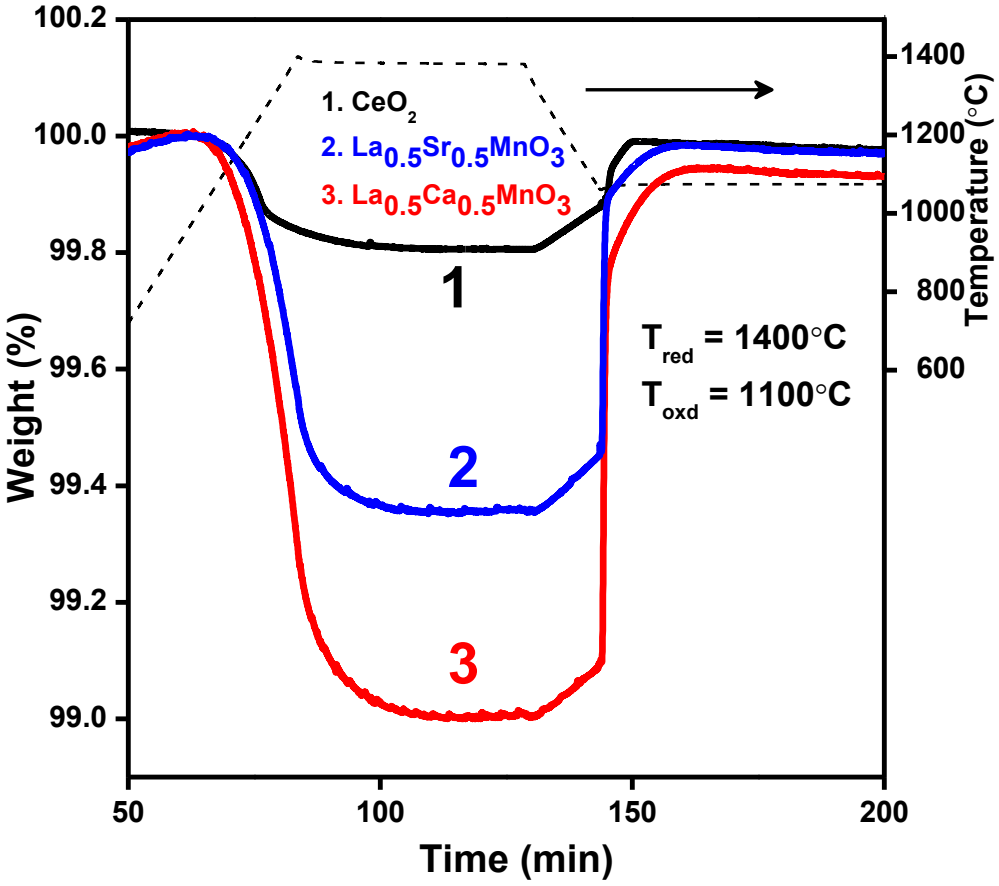

Composites	O_2 released (μmol/g)	CO produced (μmol/g)
$La_{0.5}Sr_{0.5}MnO_3$	201.3	325
$La_{0.5}Ca_{0.5}MnO_3$	**315.6**	**525**
Ceria	62.5	112

LCM 50 evolves 1.5 times and 5 times greater amount of O_2 and/or CO than LSM 50 and ceria respectively.

Sunita Dey, B. S. Naidu, A. Govindaraj and C. N. R. Rao, **Phys. Chem. Chem. Phys ,** 2015, **17**, 122-125

Thermochemical H_2Osplitting

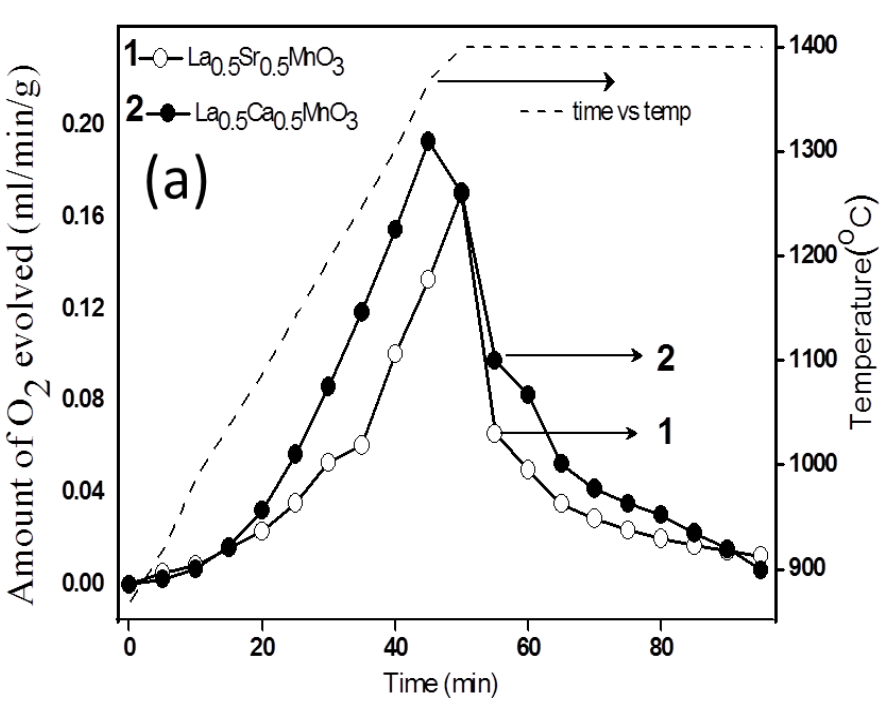

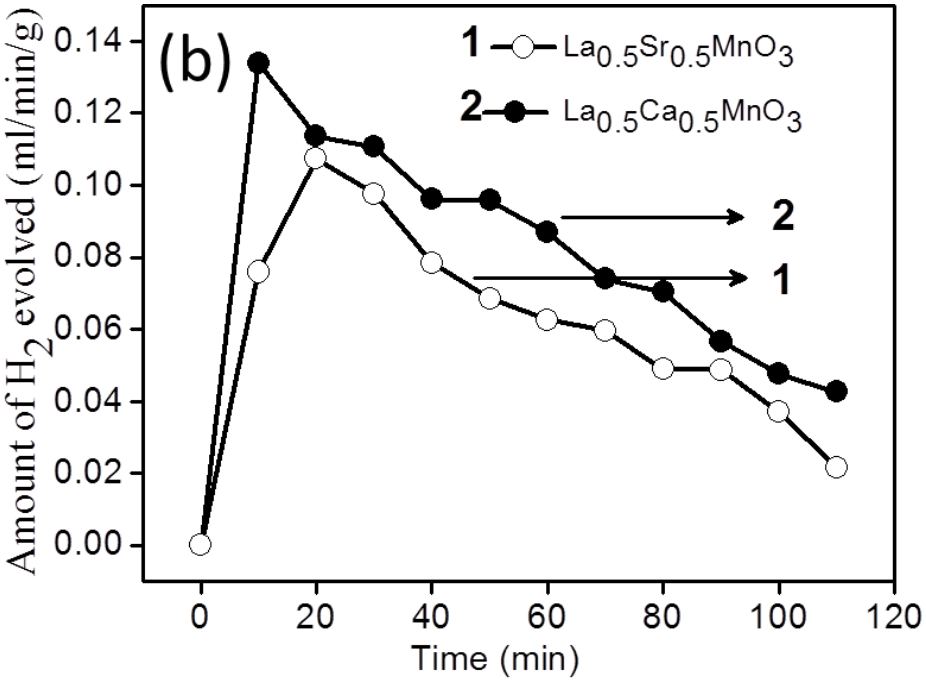

- The amount of H_2 produced by LCM 50 (407 μmol/g) is large than the LSM 50 (308 μmol/g).

Thermochemical CO_2 Splitting of $Ln_{0.5}A_{0.5}MnO_3$(Ln=lanthanide; A=Sr, Ca)

$Ln_{0.5}A_{0.5}MnO_3$

La	Nd	Sm	Gd	DY	Y

Decrease in size of Ln →

Decrease tolerance factor (τ) →

O_2 evolution of $Ln_{1/2}Sr_{1/2}MnO_3$

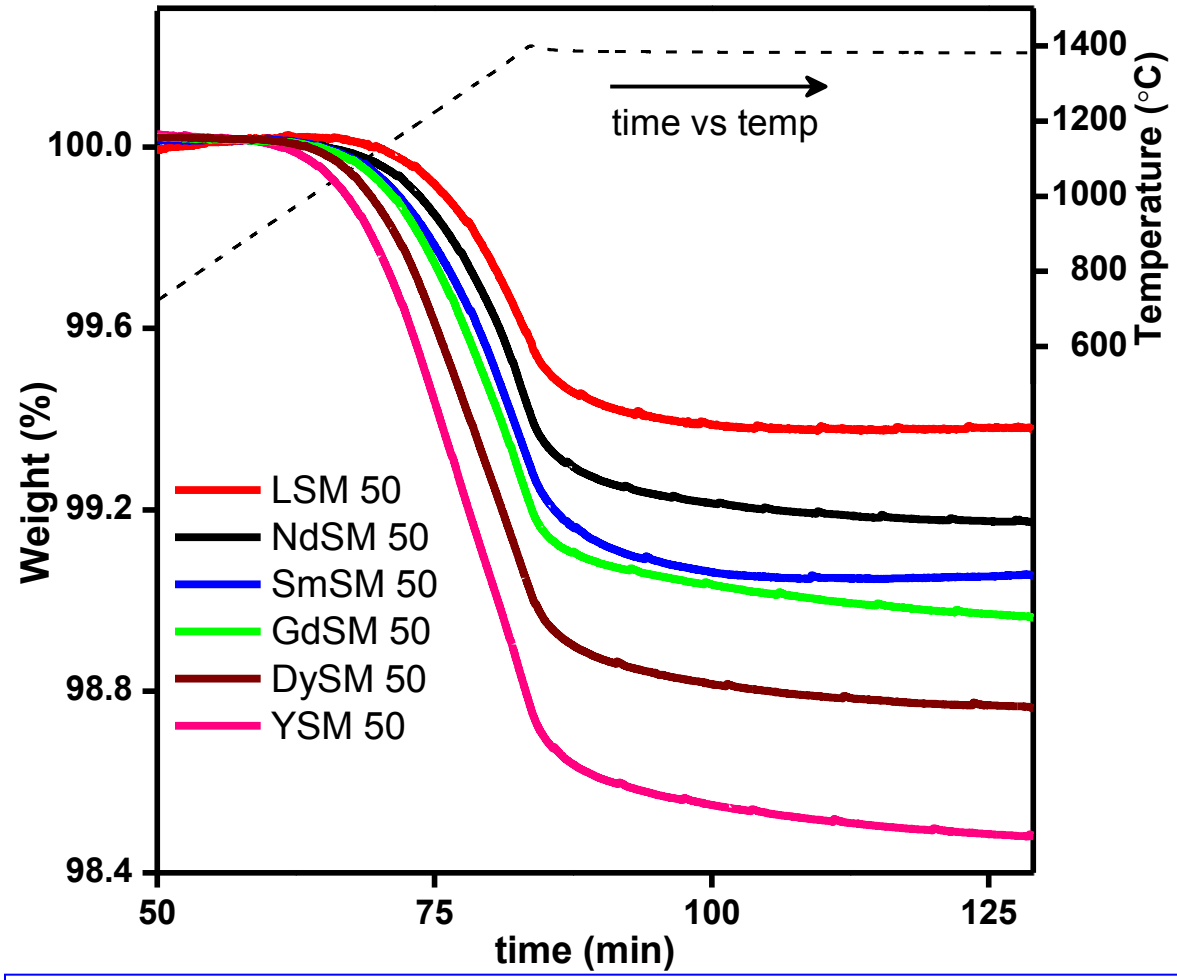

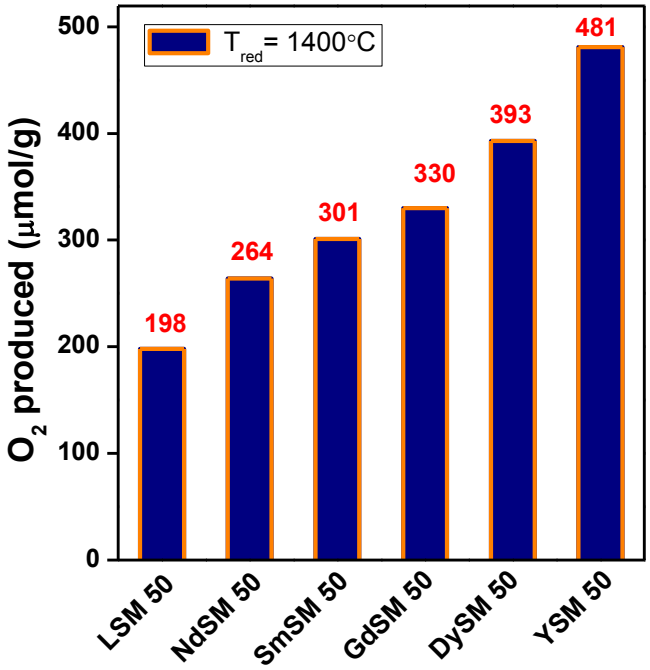

O_2 evolution increases with decreasing the size of the rare earth ions.

O_2 evolution of $Ln_{1/2}Sr_{1/2}MnO_3$

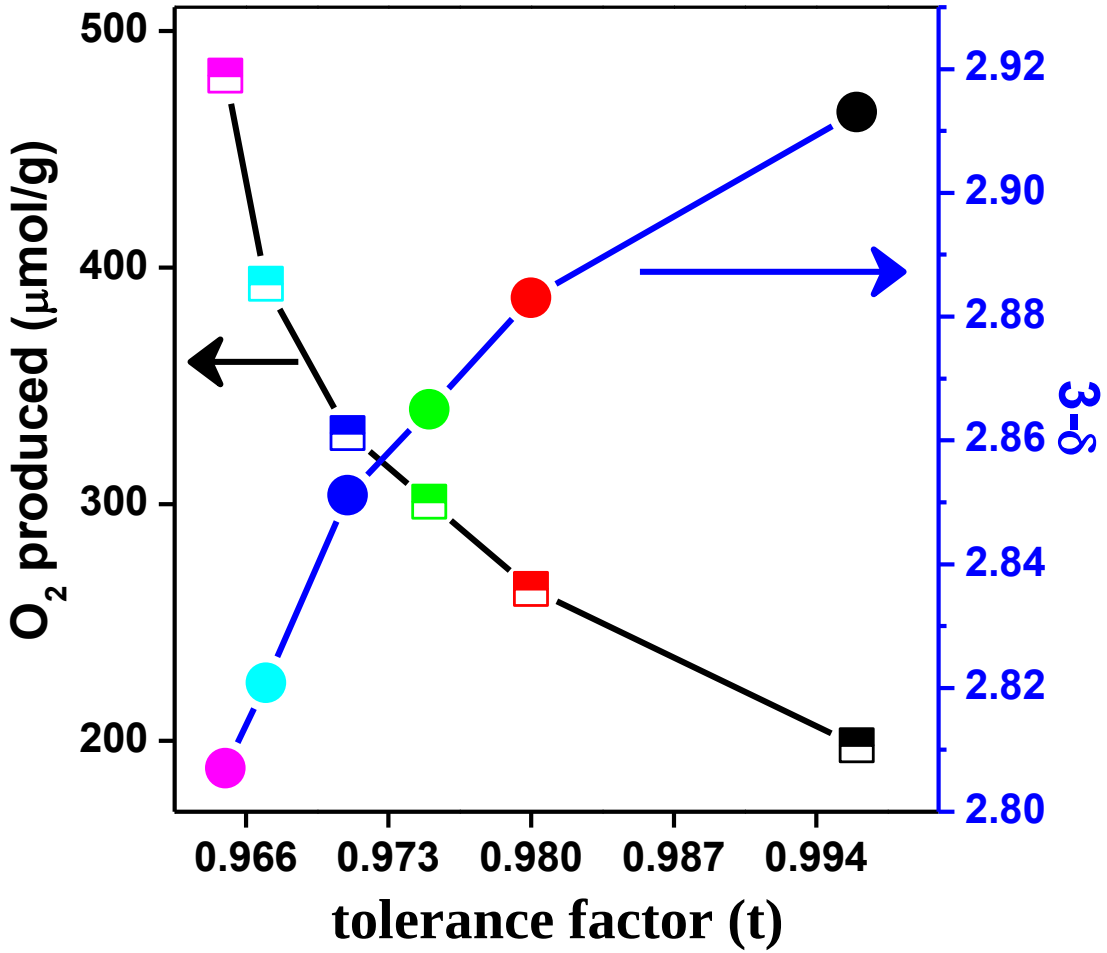

O_2 evolution increases with decreasing the tolerance factor (τ)

$Y_{0.5}Sr_{0.5}MnO_3$ shows superior O_2 production activity.

Difference in Reduction temperature

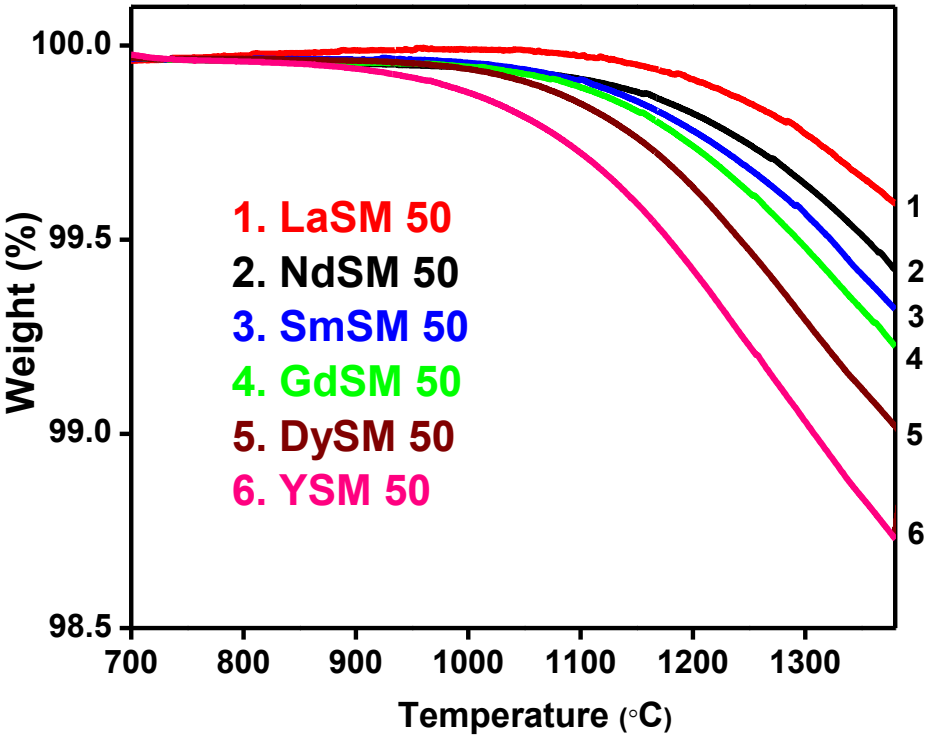

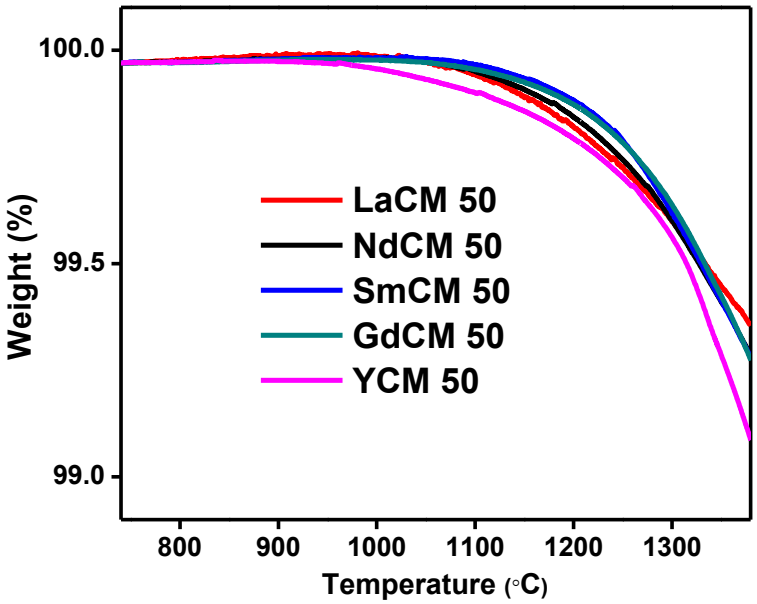

LaSM50	1050°C
YSM50	**860°C**
LaCM50	1020°C
YCM50	**970°C**

$Ln_{0.5}Sr_{0.5}MnO_3$ starts to reduce at lower temp.

Size variance (σ^2) also plays a major role ($\sigma^2_{(La, Sr)} >> \sigma^2_{(La, Ca)}$)

Remarkable performance of $Y_{1/2}Sr_{1/2}MnO_3$

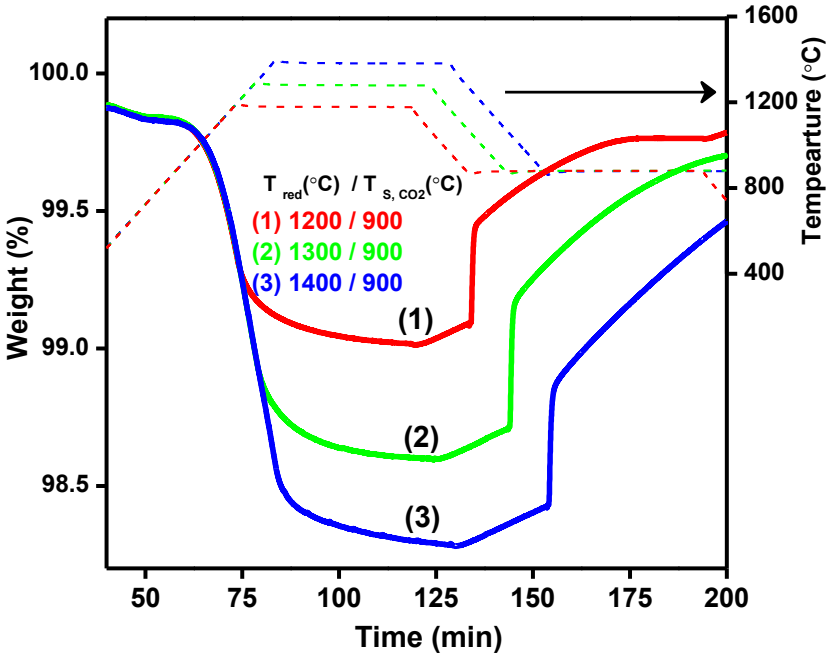

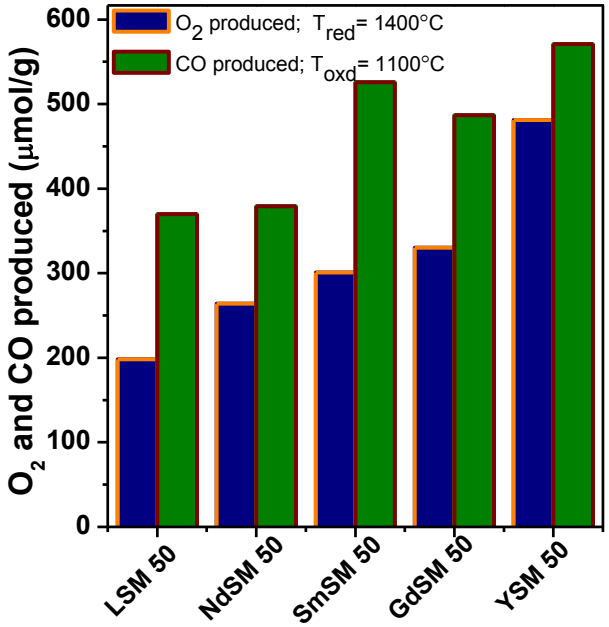

Oxidation yield of YSM 50 is less at 1100°C

Oxidation is carried out at 900°C

Materials	T_{red} (°C)	T_{oxd} (°C)	Total CO (O_2) produced (µmol/g
YSM 50	1400	900	757 (483)
YSM 50	1300	900	624 (389)
YSM 50	1200	900	418 (258)

Sunita Dey, B. S. Naidu and C. N. R. Rao, **Chem. Eur. J ,** 2015, **21**, 7077-7081.

Remarkable performance of $Y_{0.5}Sr_{0.5}MnO_3$

Material	T_{red} temp (°C)	O_2 evolved (μmol/g)	Oxidation temp (°C)	CO evolved (μmol/g)	References
$Y_{0.5}Sr_{0.5}MnO_3$	**1400**	**483**	**900**	**757**	**Present work**
$Y_{0.5}Sr_{0.5}MnO_3$	**1300**	**389**	**900**	**624**	**Present work**
$Y_{0.5}Sr_{0.5}MnO_3$	**1200**	**258**	**900**	**418**	**Present work**
$Y_{0.5}Ca_{0.5}MnO_3$	**1400**	**575**	**1100**	**671**	**Present work**
$La_{0.5}Ca_{0.5}MnO_3$	1400	315	1100	525	PCCP, 2015
$La_{0.5}Sr_{0.5}MnO_3$	1400	298	1000	298	J.Phys. Chem. C, 2014
$La_{0.6}Sr_{0.4}MnO_3$	1400	205[a)]	800	397	J.Mater. Chem. A, 2014
$La_{0.6}Sr_{0.4}Al_{0.6}Mn_{0.4}O_3$	1350	120	1000	247	Energy. Environ. Sci, 2013

Sunita Dey, B. S. Naidu and C. N. R. Rao, **Chem. Eur. J ,** 2015, **21**, 7077-7081.

Thermochemical H_2O splitting

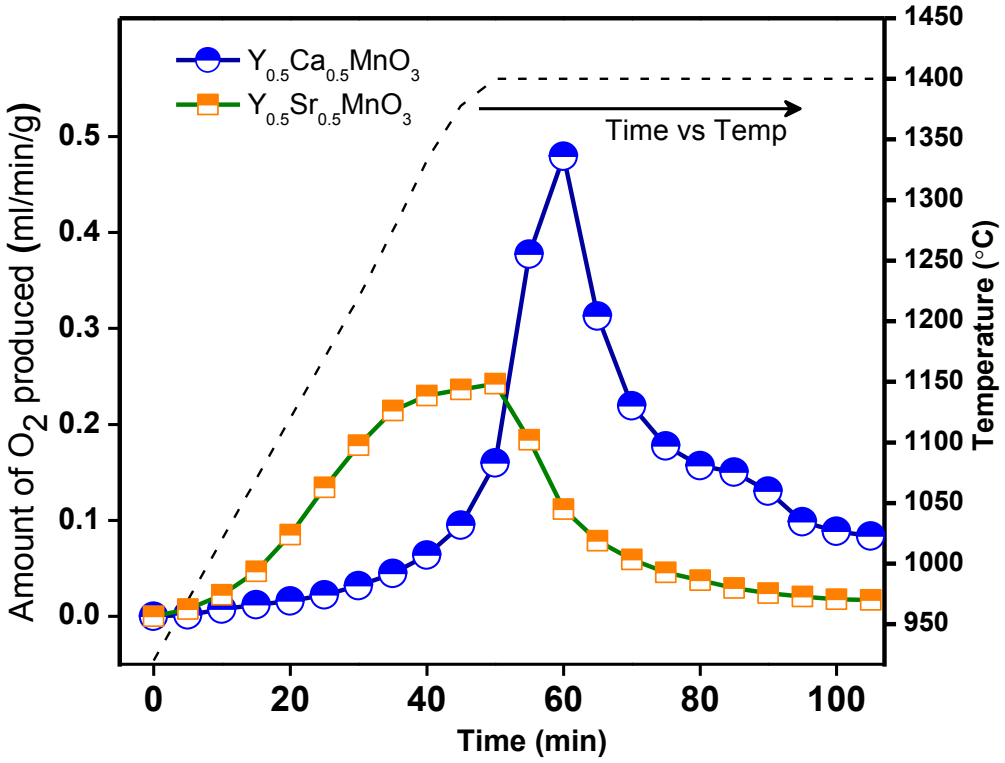

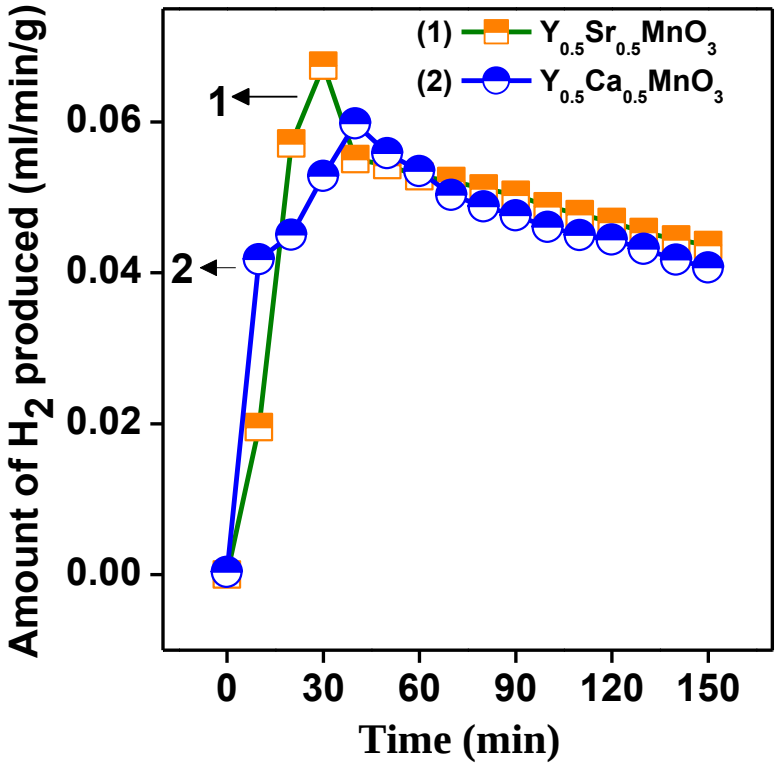

- The amount of H_2 produced by YSM 50 (320 μmol/g) is large than the YCM 50 (300 μmol/g) in 140 mins span of time.

Thermochemical H_2O splitting

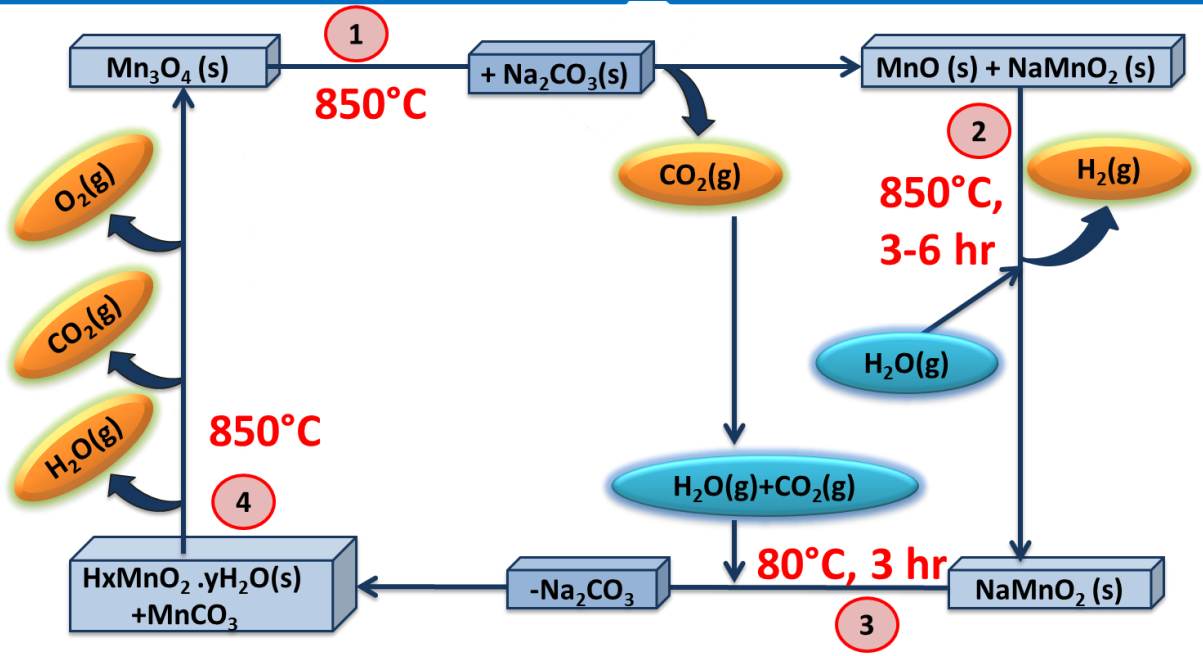

$$2Mn_3O_4 + 3Na_2CO_3 \rightarrow 4NaMnO_2(s) + 2MnO + Na_2CO_3 + 2CO_2(g) - (1)$$

$$2MnO + Na_2CO_3 + H_2O(g) \rightarrow 2NaMnO_2(s) + CO_2(g) + H_2(g) --- -(2)$$

$$6NaMnO_2(s) + ayH_2O(l) + (3+b)CO_2(g) \rightarrow 3Na_2CO_3(aq) + aH_xMnO_2.yH_2O(s) + bMnCO_3 + cMn_3O_4 -- -(3)$$

$$aH_xMnO_2.yH_2O(s) + bMnCO_3 \rightarrow (2-c)Mn_3O_4(s) + ayH_2O(g) + bCO_2(g) + 0.5O_2(g) - -(4)$$

where a+b+3c=6 and (4-x)a+2b+8c=18

Davis and Coworkers, *PNAS*, **2012,***109*, 9260

- ***Our aim :***
  1. **Lowering of reaction temperature below 850°C (steps 1 & 2)**
  2. **Increasing the H_2 evolution rate (step 2)**

Thermochemical H_2O splitting

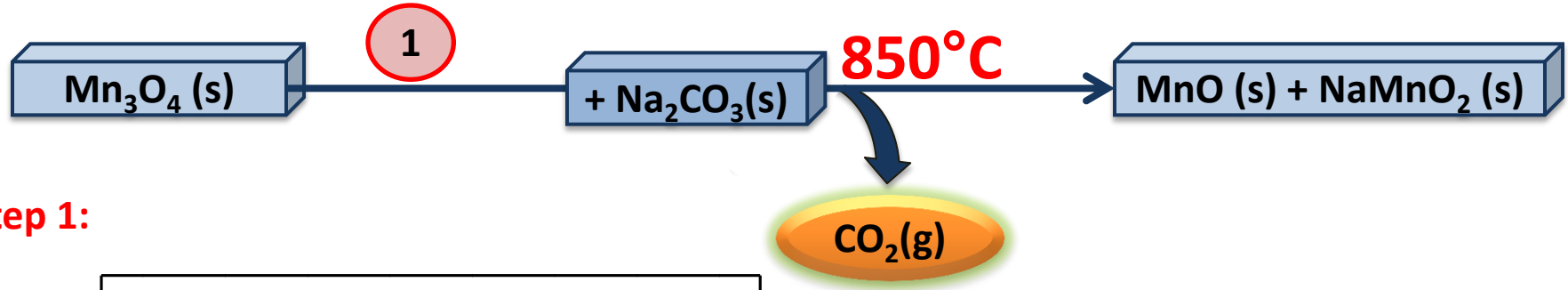

Step 1:

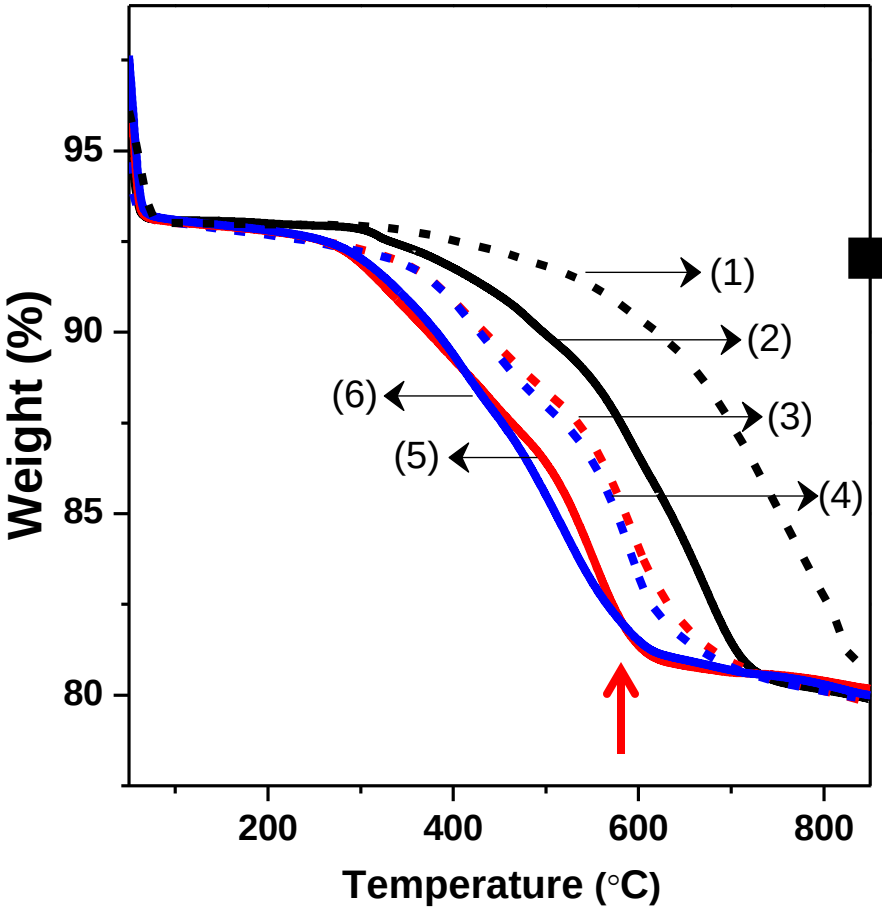

(1) Mn_3O_4-annealed+ Na_2CO_3 bulk
(2) Mn_3O_4-commercial+ Na_2CO_3 bulk
(3) Mn_3O_4-30 mins ball milled+ Na_2CO_3 bulk
(4) Mn_3O_4-60 mins ball milled+ Na_2CO_3 bulk
(5) (Mn_3O_4 + Na_2CO_3)-30 mins ball milled
(6) (Mn_3O_4 + Na_2CO_3) -60 mins ball milled

CO_2 evolution temperature decreases upto 600°C with the use of nanoparticles of both Mn_3O_4 + Na_2CO_3.

Sunita Dey, S. Rajesh and C. N. R. Rao, **J. Mater. Chem. A,** 2016, DOI: 10.1039/c6ta06271g

Thermochemical H_2O splitting

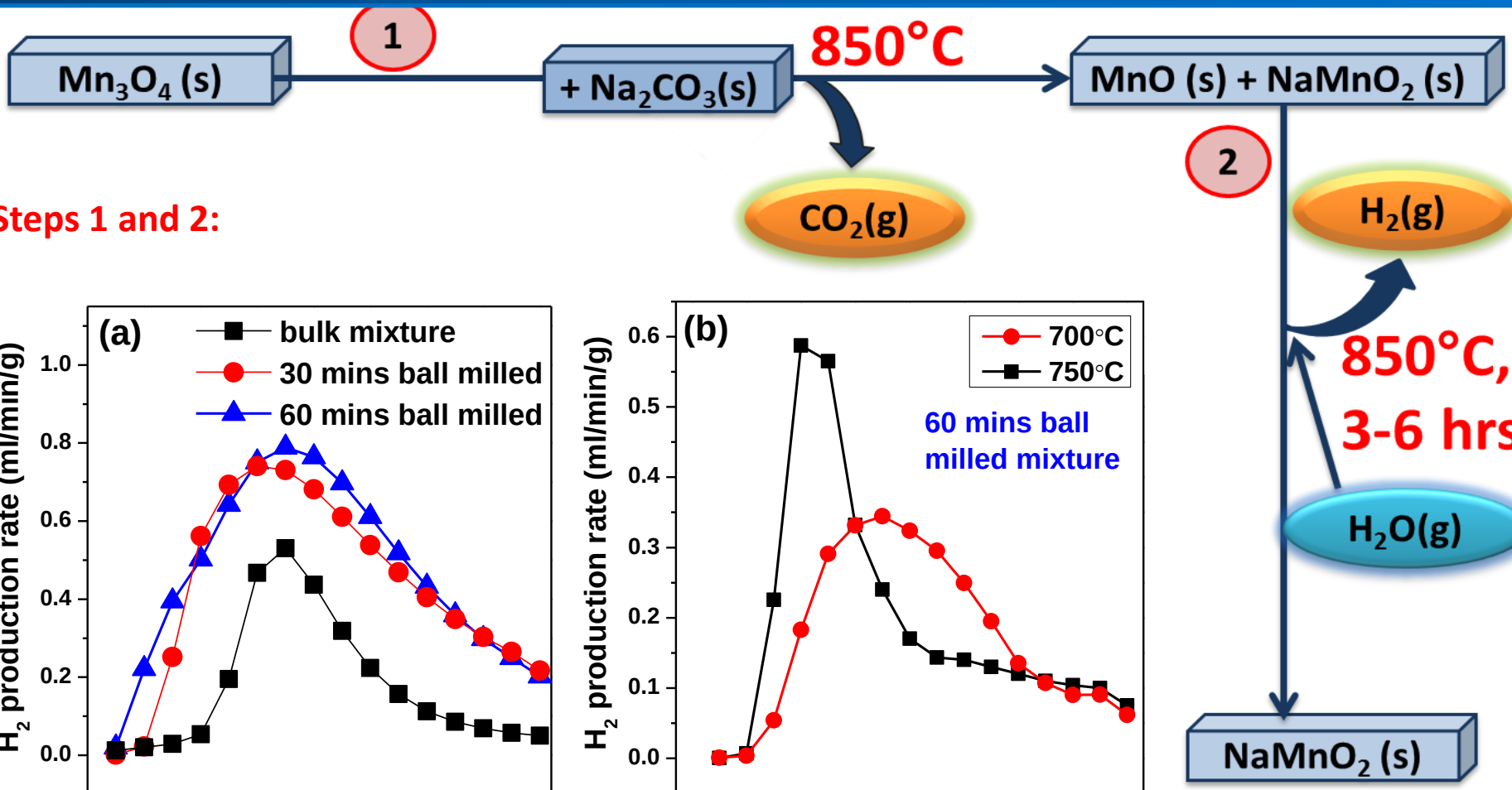

Steps 1 and 2:

1. H_2 evolution rate increases
2. H_2 evolution temperature decreases upto 750°C and 700°C

Sunita Dey, S. Rajesh and C. N. R. Rao, **J. Mater. Chem. A,** 2016, DOI: 10.1039/c6ta06271g

Why not electrolysis of water using solar PV?

- Problem of over potential
- Need of a catalyst other than Pt
- BC_XN_Y?

Electrochemical Hydrogen Evolution

Selection of catalyst

i_0 as a function of the ΔG_H* for various catalysts

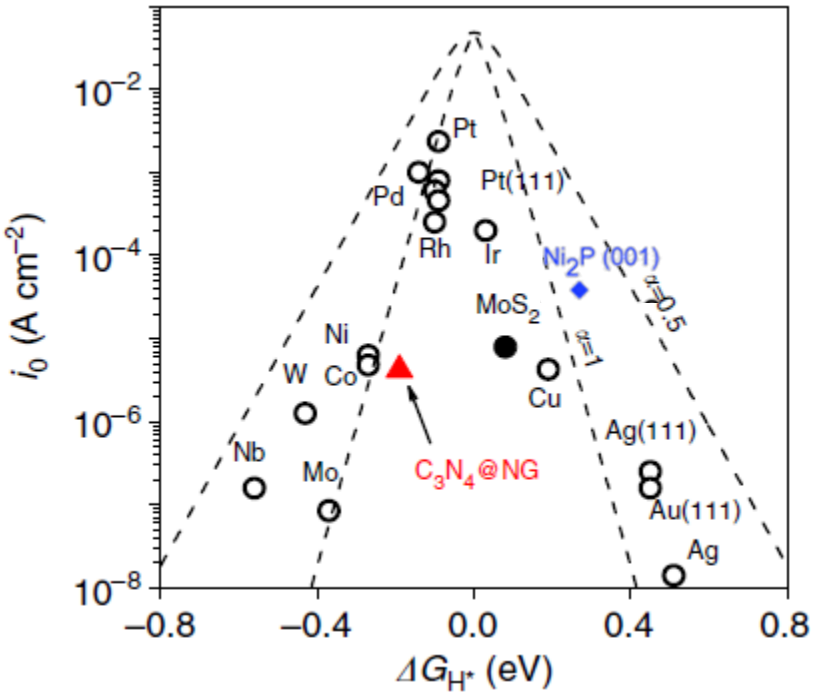

Volcano Plot

Limitations

- Innate overpotential.
- Durability in harsh acidic and basic medium.
- High cost and scarcity of precious metals.

Low cost metal free electrocatalysts

- Heteroatom doping – Active surface sites for H^+ adsorption
- Enhanced conductivity – low charge transfer resistance
- Examples- modified MoS_2 based, C_3N_4@NG , etc.

$B_XC_YN_Z$: ???

Y. Zheng, Y. Jiao, Y. Zhu, L. H. Li, Y. Han, Y. Chen, A. Du, M. Jaroniec and S. Z. Qiao, ***Nat. Commun.***, *2014*, ***5.***

Electrochemical Hydrogen Evolution

Linear Sweep Voltametry

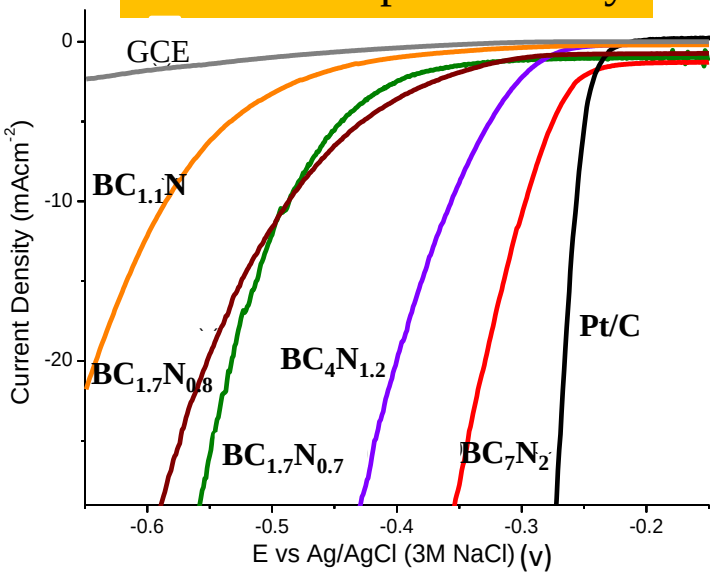

Stability after 1000 cycles

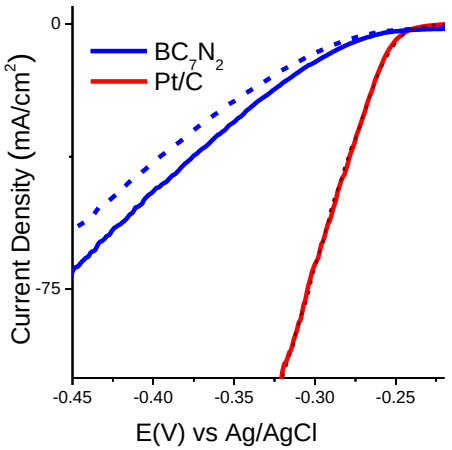

Stability @ 20 mA/cm^2

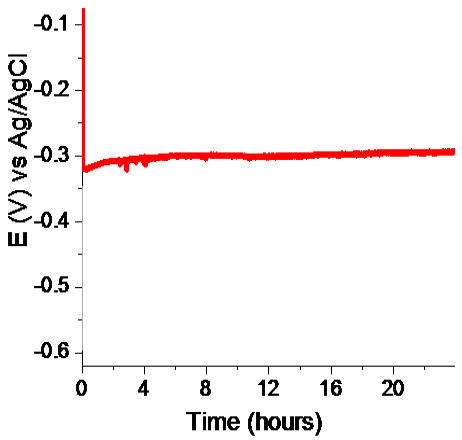

Electrochemical Impedance Spectroscopy

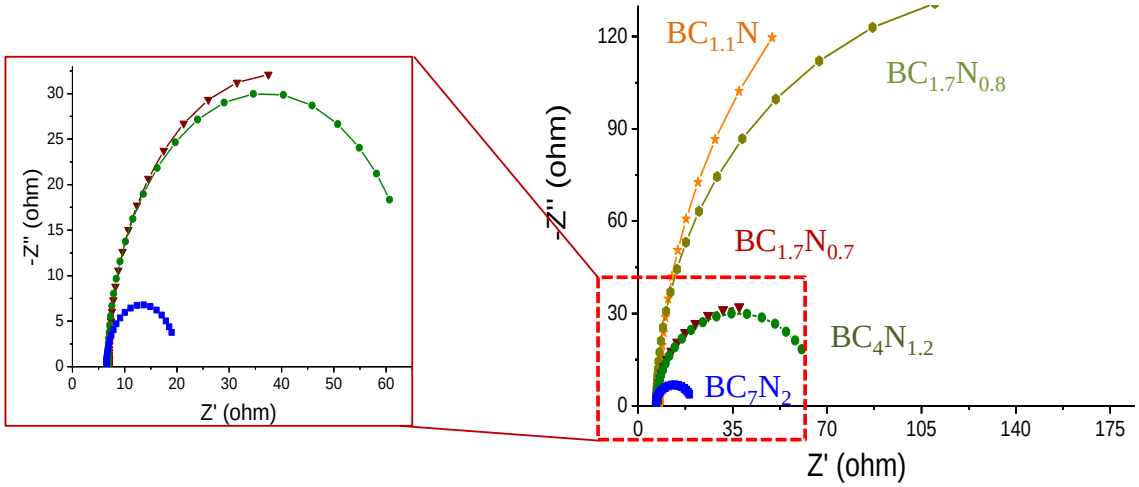

Tafel slope

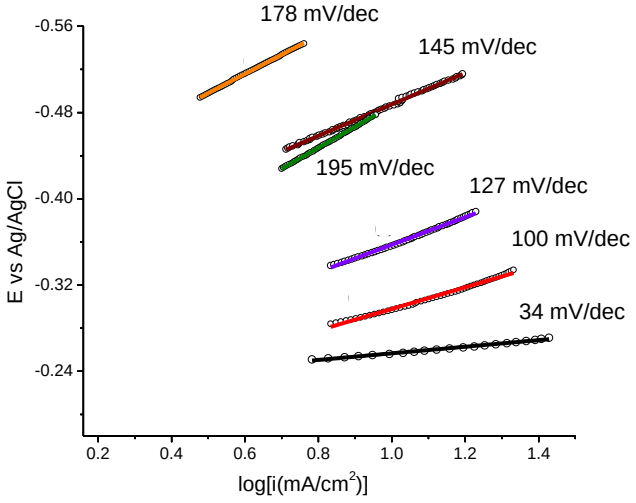

M. Chhetri, S. Maitra, H. Chakraborty, U. V. Waghmare, C. N. R. Rao, **Energy Environ. Sci.,** 2016, **9**, 95.

Comparative study and literature

Summary of electrocatalytic activity

Sample	BET (m^2/g)	Onset[(a)] (mV) vs Ag/AgCl	η@10 mA/cm^2 (a)	η@20 mA/cm^2 (a)	Tafel Slope	I_o (A/cm^2)	R_{ct}	C_{dl} (mF/cm^2)
BC_7N_2	1950	-284	-298 mV	-330 mV	100 mV/dec	5.1×10^{-5}	13.6 Ω	0.108
$BC_4N_{1.2}$	1635	-314	-357 mV	-401 mV	127 mV/dec	3.2×10^{-5}	60.1 Ω	0.103
$BC_{1.7}N_{0.7}$	1470	-451	-487 mV	-642 mV	195 mV/dec	1.09×10^{-5}	64.3 Ω	0.033
$BC_{1.7}N_{0.8}$	1241	-444	-487 mV	-533 mV	145 mV/dec	9.1×10^{-6}	268.9 Ω	0.022
$BC_{1.1}N$	1580	-428	-586 mV	-542 mV	178 mV/dec	4.4×10^{-6}	384.6 Ω	0.020
Pt/C	--	-230	-250 mV	-266 mV	34 mV/dec	--	--	--

Catalyst	Onset (mV) Vs RHE	η@10mA/cm² vs RHE	Tafel slope (mV/dec)
3D-MoS_2/N-GAs	-236	-261	230
N-MPG	-220	-239	109
C_3N_4@NG	-180	-240	51
g-C_3N_4 nanoribbons	-80	-200	54
N-graphene on Si	-200	-260	74
MoS_2/RGO hybrid	-100	-150	41
Mo_2C/C nanocomposite	-100	-270@5mA/cm^2	110
BC_7N_2	-56	-70	100

[(a)]Against RHE the values can be converted by adding 227.7 mV, following the equation for calibration against, $E_{(RHE)} = E^{o}_{(Ag/AgCl,\ 3\ M\ NaCl)} + E_{(Ag/AgCl,\ 3\ M\ NaCl)} + 0.059*pH$

Faradaic Efficiency

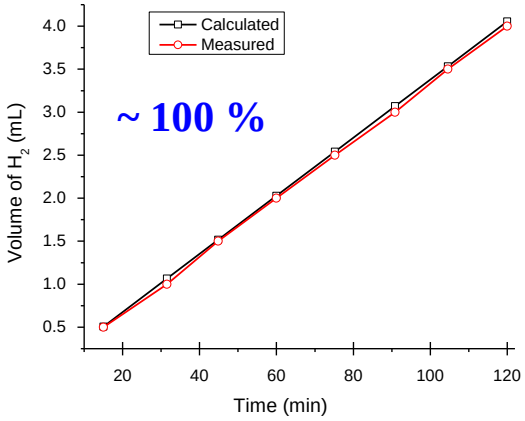

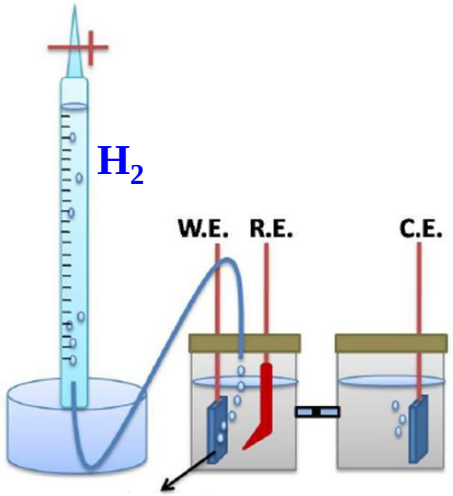

BC_7N_2

First Principles calculations

BC_7N_2

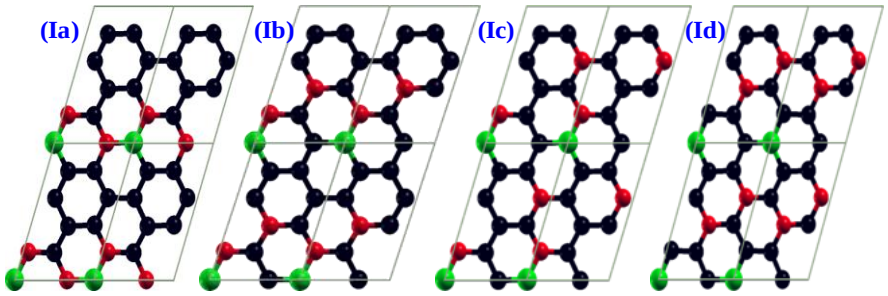

$B_2C_2N_2$

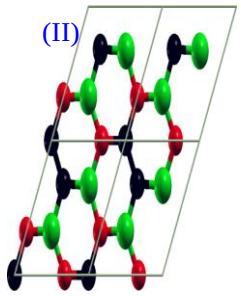

BC_8N

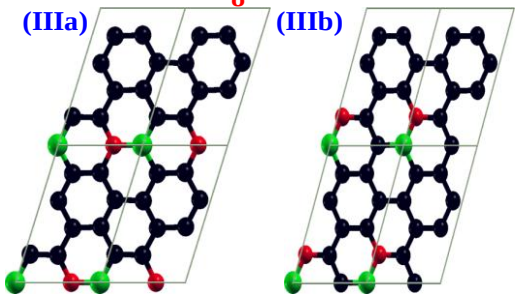

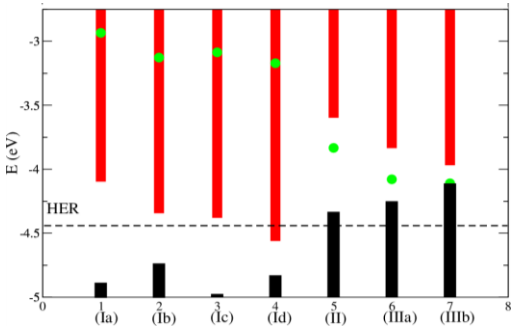

Composition dependant HER activity

Presence of two Nitrogen

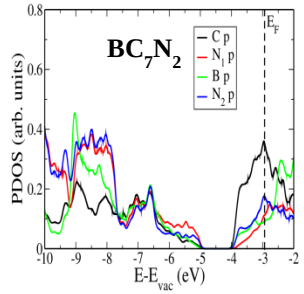

Presence of Boron

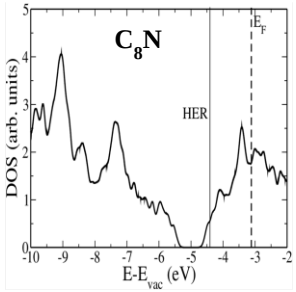

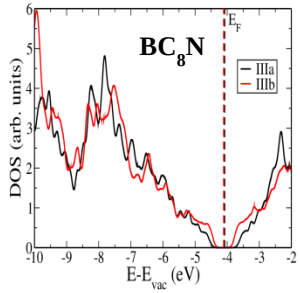

Configuration	Relative Energy E(config)-E(lowest) (eV/supercell)	VBM (eV)	CBM (eV)	E_F (eV)	DoS(E_F) (arb. units)
Ia	0	-4.888	-4.094	-2.934	1.747
Ib	1.076	-4.738	-4.341	-3.127	1.312
Ic	0.819	-4.976	-4.377	-3.086	1.143
Id	2.078	-4.830	-4.558	-3.171	1.193
II	-	-4.112	-3.595	-3.833	0
IIIa	0	-4.335	-3.832	-4.078	0
IIIb	0.132	-4.252	-3.966	-4.109	0

Conclusion and Highlights

1. First report on the Efficacy of borocarbonitride sheets as an excellent low-cost, metal-free catalyst for hydrogen generation.

2. Carbon-rich BC_7N_2 shows the best activity with a performance superior to that of other non-precious metal electrocatalyst.

2. Faradaic Efficiency is ~100%, showing almost no deviation from the theoretically calculated value of the volume of hydrogen evolved.

3. Theoretical studies show that substitution of B and N in equal concentrations opens up a gap, with the valence band unfavorably located relative to the HER potential.

4. Substitution of excess N results in the population of the conduction bands with electrons and shifts the valence and conduction bands to lower energy and favors the alignment of bands to facilitate electrocatalysis.

5. The optimal composition should be (a) Carbon-rich (hence low in B and N), (b) excess in N (relative to B).

6. Interplay of the relative ratio betwee B & N can afford entropic stability and an adequate number of active sites for HER,

M. Chhetri, S. Maitra, H. Chakraborty, U. V. Waghmare, C. N. R. Rao, **Energy Environ. Sci.,** 2016, **9**, 95.

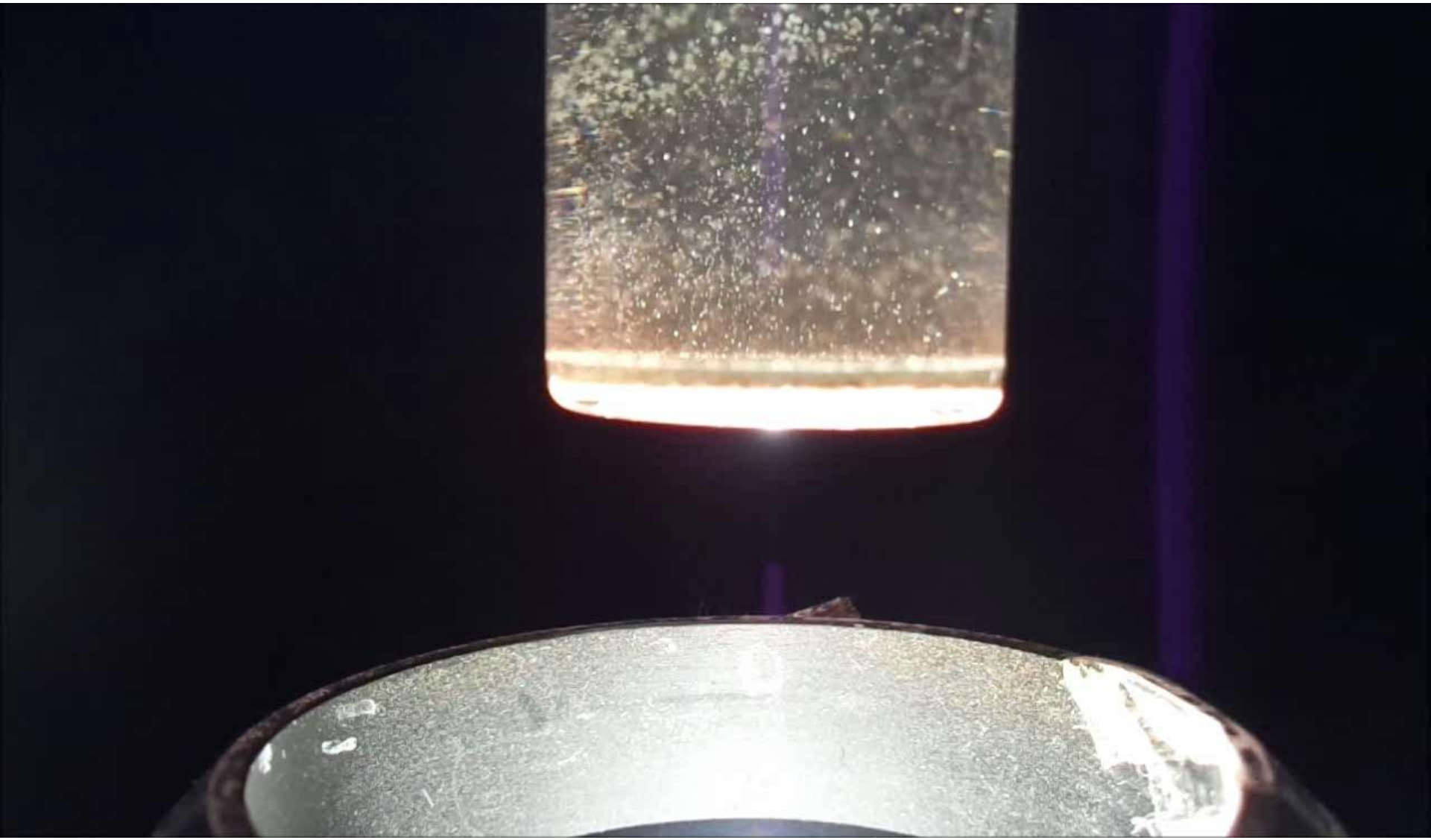

OUTLOOK